

UNIVERSITA' DEGLI STUDI DI SASSARI

DOTTORATO DI RICERCA

"Biochimica, Biologia e Biotecnologie Molecolari"

*Coordinatore:* Prof. Bruno Masala

Ciclo XXI

“AORTIC AND PULMONARY BIOPROSTHETIC HEART VALVES:  
AN INSIGHT ON GLYCOSAMINOGLYCAN DISTRIBUTION AND  
FINE STRUCTURE IN DECELLULARIZED PORCINE SCAFFOLDS  
FOR TISSUE ENGINEERING PURPOSES.”

Tutore

Prof.ssa Marilena Formato

Correlatore

Dott. Antonio J. Lepedda

Dipartimento di Scienze Fisiologiche, Biochimiche e Cellulari

Dottorando

Dott. Antonio Cigliano

Anno Accademico 2007-2008





UNIVERSITA' DEGLI STUDI DI SASSARI

DOTTORATO DI RICERCA

"Biochimica, Biologia e Biotecnologie Molecolari"

*Coordinatore:* Prof. Bruno Masala

Ciclo XXI

“AORTIC AND PULMONARY BIOPROSTHETIC HEART VALVES:  
AN INSIGHT ON GLYCOSAMINOGLYCAN DISTRIBUTION AND  
FINE STRUCTURE IN DECELLULARIZED PORCINE SCAFFOLDS  
FOR TISSUE ENGINEERING PURPOSES.”

Tutore

Prof.ssa Marilena Formato

Correlatore

Dott. Antonio J. Lepedda

Dipartimento di Scienze Fisiologiche, Biochimiche e Cellulari

Dottorando

Dott. Antonio Cigliano

Anno Accademico 2007-2008

	<b>Index</b>
<b>1. Introduction</b>	<b>page 1</b>
1.1 Extracellular Matrix (ECM)	2
1.1.1 Glycosaminoglycans (GAG)	3
1.1.1.1 Hyaluronan (HA)	5
1.1.1.2 Chondroitin Sulfate Isomers (C4S, C6S, DS)	5
1.1.1.3 Heparin (HE) and Heparan Sulfate (HS)	6
1.1.1.4 Keratan Sulfate	6
1.1.2 Proteoglycans (PG)	6
1.1.3 Collagens	9
1.1.4 Elastic fibers	9
1.2 Cardiac valves	10
1.2.1 Morphology	10
1.2.2 Heart valve substitutes	12
<b>2. Aim of this work</b>	<b>18</b>
<b>3. Materials and methods</b>	<b>20</b>
3.1 Tissue analysis	20
3.2 Extraction and purification of total GAGs	20
3.3 Acetate cellulose electrophoresis	21
3.4 Depolymerization of the GAGs	22
3.5 Fluorotagging with 2-Aminoacridone (AMAC)	22
3.6 FACE analysis	23
3.7 CS calibration curve and statistical analysis	23
<b>4. Results and Discussion</b>	<b>25</b>
<b>5. Conclusions</b>	<b>29</b>
<b>Figures and tables</b>	<b>31</b>
<b>References</b>	<b>I-IX</b>

## 1. Introduction

In the past, heart valves were considered simple structures whose contribution to the unidirectional flow of blood was a merely passive movement in response to pressure gradients across the valve. It is now becoming apparent, however, that the heart valves have a more complex structure, consisting of vital and dynamic tissues composed of cells and extracellular matrix (ECM), specialized for the micro-environment in which they are placed, that respond and remodel in response to changes in local mechanical forces<sup>1,2</sup>. Cardiac valves are dynamic structures with a complex architecture highly specialized, consisting of an avascular, semi-fluid and deformable matrix enriched in Proteoglycans (PGs), Glycosaminoglycans (GAGs), collagen and elastic fibers. All these molecules give unique physical and mechanical features conferring to the valves the ability to bear high mechanical stresses during the normal cardiac cycle. GAGs into the ECM form a gel-like ground on which other molecules are deposited, forming permanent cross-links and interacting between them to make a network that limit the structural solicitations due to bending and shearing stresses during the cardiac cycle. Heart valve disease has a devastating impact worldwide; every year numerous heart valve replacement procedures are performed (**Fig. 1.1**).

Typical valve substitutes are mechanical prostheses and bioprostheses distinct in “Xenograft” and “Homograft”. During the last 15 years, tissue engineering (TE) approaches emerged in response to limitations associated with tissue and organ transplantation and with the scarcity of available donor tissue. It is believed that TE could assure the post implant recovery of normal function of the native valve. TE approaches to the construction of a heart valve, or any other tissue or organ, typically rely on three essential components: (1) cells, (2) scaffolds, designed to maintain the cells in a three-dimensional environment at the implantation site, and (3) signals that guide the gene expression and ECM production of the cells during tissue development<sup>2</sup>. Tissue engineering, defined as the regeneration of tissue by cell transplantation with the aid of supporting structures, is thought to overcome the obstacles of artificial tissue prostheses in cardiovascular surgery. Two major principles are followed in matrix research: (1) development of biodegradable polymer constructs emulating the initial anatomical structure; and (2) decellularization of preformed tissue, such as heart valves or blood vessels is under investigation. Decellularization generally refers to the removal of cells and cellular remnants while leaving a biological material composed essentially of extracellular matrix (ECM) components. The organization and remodeling of ECM is partially controlled by mechanical stresses and strains. GAGs and PGs are essential ECM components in valve tissues and have been shown to be segregated according to the type of loading that distinct regions experience<sup>101</sup>. The goal of the

---

Antonio Cigliano, “Aortic and pulmonary bioprosthetic heart valves: an insight on glycosaminoglycan distribution and fine structure in decellularized porcine scaffolds for tissue engineering purposes” Dottorato in Biochimica, Biologia e Biotecnologie Molecolari – Università degli studi di Sassari.

current study was to provide insight onto decellularization approach to TEHV. The comprehension of which are the micro-structural effects on Glycosaminoglycans content caused by decellularization of the valve tissues and establishing functional limits are essential to the future development of a functional TEHV.

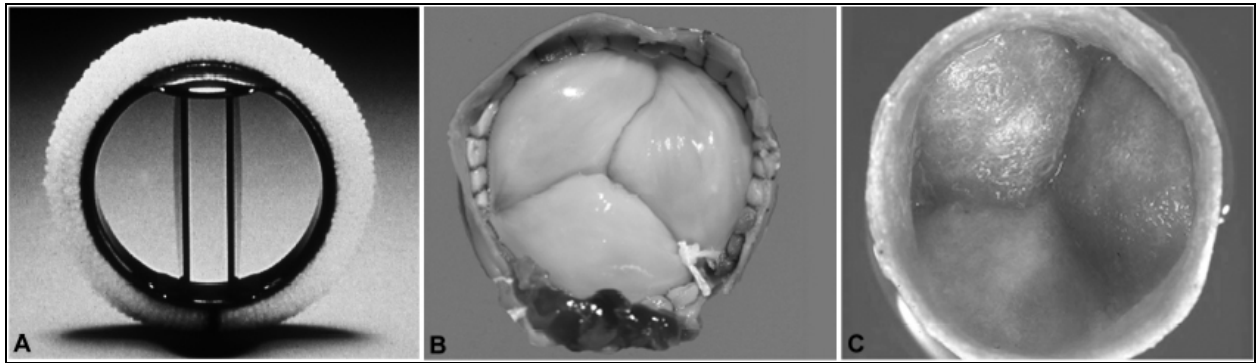


*Fig. 1.1* - (A) Mechanical prosthesis. (B) Bioprosthesis. (C) Tissue engineered. (Hoerstrup et al., Circulation 2002).

### *1.1 Extracellular Matrix (ECM)*

Most cells in multicellular organisms are in contact with an intricate network of interacting extracellular collagens, PGs and adhesion proteins, as well as growth factors, chemokines and cytokines. Together, these components constitute the extracellular matrix (ECM). Many ECM proteins form large families and additional events, such as alternative splicing, proteolytic processing and post-translational events, increase the number of unique structures and expand the functions of these large, multifunctional molecules<sup>3</sup>. The vascular ECM is a complex, dynamic, highly specialized and critical component of this tissue; it is characterized by a fibrillar component, containing mainly elastic and collagen fibers organized in supramolecular structures, and by an amorphous component forming a complex colloidal multiphase system distinct in an aqueous phase, in which are solubilized the electrolytes, and in a dispersed phase in which are present enzymes and the other molecules described above. These components interact and cross-link to form a biomechanically active polymer network that imparts tensile strength, elastic recoil, compressibility and viscoelasticity to vascular wall<sup>4-6</sup>. This network interacts with vascular cells and participates in the regulation of cell adhesion, migration and proliferation during vascular development and disease. Furthermore, components of the ECM bind plasma proteins, growth factors, cytokines and enzymes and these interactions modulate arterial wall metabolism. Thus, the vascular ECM not only maintains vascular wall structure but also regulates key events in vascular physiology<sup>4,7,8</sup>. The ECM scaffold-like provides tensile strength

Antonio Cigliano, "Aortic and pulmonary bioprosthetic heart valves: an insight on glycosaminoglycan distribution and fine structure in decellularized porcine scaffolds for tissue engineering purposes" Dottorato in Biochimica, Biologia e Biotecnologie Molecolari – Università degli studi di Sassari.

and support suitable for tissue repairing, renewing and remodelling. The ECM as a fibers and soluble polymers network is evolved to stress absorber and maintain its shape; the composition of the ECM is controlled by the coordinate and differential regulation of synthesis and turnover of each of its components<sup>4</sup>. Such differential regulation creates differences in the composition of the vascular ECM during vascular development, between different vascular beds and in different forms of vascular disease<sup>9,10</sup>. For example, each layer of the vessel wall: *Intima*, *Media* and *Adventitia* has a different ECM composition. An ECM rich in fibrillar collagen, as is found in the adventitia, will impart stiffness and rigidity, whereas a layer enriched in PGs and hyaluronan, as found in the intima, is more viscoelastic and compressible. Maintaining the appropriate balance of the components in each layer is critical for maintaining vascular wall integrity and resisting rupture and hemorrhage<sup>4</sup>.

### 1.1.1 Glycosaminoglycans (GAGs)

Complex polysaccharides are primary constituents of every eukaryotic cell surface and extracellular environment. GAGs are linear acidic polysaccharides containing a variable number of repeating disaccharide subunits, each consisting of an hexuronic acid linked to an hexosamine extensively *N*- and *O*-sulfated. There are four classes of GAGs based on their different chemical structures<sup>11</sup>: [1] chondroitin sulfate (CS) and dermatan sulfate (DS), [2] heparin (HE) and heparan sulfate (HS), [3] hyaluronan (HA), and [4] keratan sulfate (KS). The disaccharide units of the polymers are composed of an hexosamine often *N*-acetylated, Glucosamine (GlcN or GlcNac) or Galactosamine (GalN or GalNac), and an hexuronic acid, Glucuronic Acid (GlcA) or after epimerization at the C-5, Iduronic Acid (IdoA), linked by  $\beta(1,3)$  or  $\beta(1,4)$  glycosidic linkages<sup>12</sup>. GAGs adopt an extended conformation, attract cations, and bind water. Hydrated GAG gels enable joints and tissues to absorb large pressure changes. They are usually covalently linked at the reducing end to core proteins (PG) through an O-glycosidic linkage to a serine residue. The synthesis of GAGs takes place in the Golgi apparatus, and requires a host of nucleotide sugar transporters and glycosyltransferases<sup>13</sup>. A wide range of protein cores serve as acceptors for the initiation and polymerization of GAG chains. Serine is the anchor site in the protein for xylose, the first monosaccharide in GAG chains, to be attached through the action of a xylosyltransferase. The exceptions are keratan sulphate and hyaluronan. Keratan sulphate chains are linked to proteins either through GlcNac–asparagines or GalNac–serine/threonine linkages. Hyaluronan is synthesized as a GAG by HA synthases at the plasma membrane without covalent binding to a protein core<sup>14</sup>. The serine attachment site for GAGs polymerization is typically located in Ser-Gly dipeptide or repeating sequences with flanking acidic amino acids.

---

Antonio Cigliano, "Aortic and pulmonary bioprosthetic heart valves: an insight on glycosaminoglycan distribution and fine structure in decellularized porcine scaffolds for tissue engineering purposes" Dottorato in Biochimica, Biologia e Biotecnologie Molecolari – Università degli studi di Sassari.

GAG synthesis is initiated by sequential addition of four monosaccharides forming the so called linker tetrasaccharide: GlcA $\beta$ 1-3Gal $\beta$ 1-3Gal $\beta$ 1-4Xyl $\beta$ 1-O-(Ser). The galactose units are transferred from UDP-galactose to the initiated chain by galactosyltransferase I and II, respectively. The last member of the linker unit is glucuronic acid (GlcA), transferred from UDP-GlcA by the enzyme glucuronosyltransferase I<sup>14-17</sup>. The growing GAG chains are modified at various positions characterizing and determining their biological roles (**Fig. 1.2**). These post-translational modifications involve length chain, epimerization of GlcA to IdoA by C-5-uronosyl epimerase, and charge density due to O-sulphation in various positions both in the hexosamine units and the IdoA units, and occasionally in the GlcA units, through the actions of defined sulphotransferases. There are several specific sulphotransferases that have been identified, responsible for the transfer of sulphate units from the activated sulphate donor adenosine 3'-phosphate 5'-phosphosulphate (PAPS) to defined positions in the different types of GAG chains<sup>15-17</sup>. The chemical heterogeneity of GAGs in terms of their sulfation pattern and backbone chemical structure depends on the expression of these enzymes, and their tissue-specific isoforms and substrates. In ECM, PGs and GAGs, in addition to their structural role, participate in many physiologic and pathologic processes, such as cell migration, differentiation, cell adhesion and communication<sup>18-20</sup>, development of nervous system<sup>21</sup>, angiogenesis<sup>22,23</sup> and embryogenesis<sup>24,25</sup>, atherosclerosis, cancer and microbial pathogenesis<sup>26-29</sup>. Chemical heterogeneity and other local variables in GAG chains allows specific ionic interactions with growth factors, cytokines, enzymes and other ECM molecules.

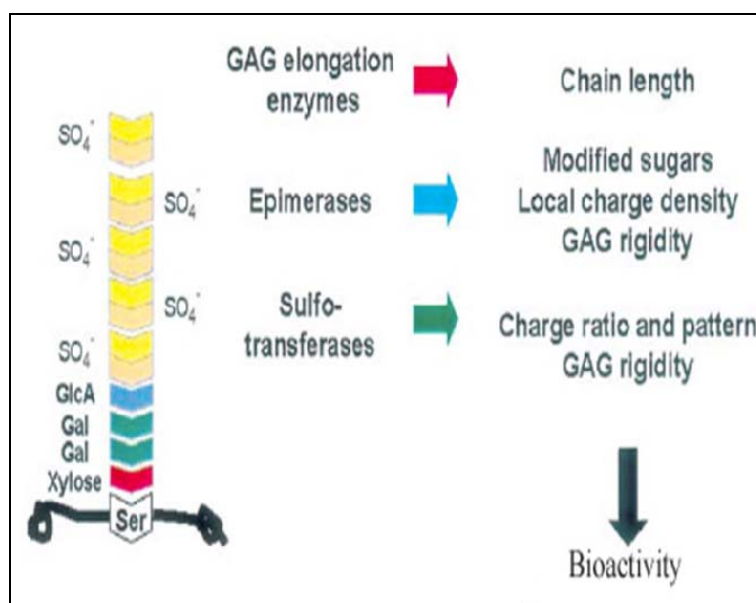


**Fig. 1.2** - Post-translational events regarding the chemical heterogeneity exhibited by GAG molecules during their synthesis.



### 1.1.1.1 Hyaluronan (HA)

Hyaluronan is an ubiquitous glycosaminoglycan synthesized as a large, negatively charged, unbranched polymer with diverse biological roles and a high molecular mass comprised solely of a repeating disaccharide of GlcA and GlcNAc linked by alternate  $\beta$ 1-3 and  $\beta$ 1-4 linkages that, unlike other GAGs, is neither sulfated nor attached to a core protein. This polysaccharide consists of 2,000–25,000 disaccharides, which corresponds to polysaccharides with relative molecular masses of  $10^6$ – $10^7$  Da and polymer lengths of 2–25  $\mu\text{m}$ <sup>31</sup>. The hyaluronan molecule in solution can be pictured as a highly organized extended dynamic coil that can undergo sharp kinks, bends and folds while still maintaining distinctive hydrogen-bond conformation<sup>32</sup>. It displays intriguing viscoelastic and conformational features, although it has a relatively simple regular structure. The lack of any chemical variation in the linear chain and its conformational flexibility make HA a versatile molecule that can form a variety of periodic multi-molecular structures through its interaction with specific HA-binding proteins, known as hyaladherins. It is thought that these capture, stabilize, and propagate particular conformations of the polysaccharide leading to HA–protein complexes with different architectures and specific functional activities<sup>30</sup>. Hyaluronan has remarkable hydrodynamic characteristics, especially in terms of its viscosity and its ability to retain water. It therefore has an important role in tissue homeostasis and biomechanical integrity, and these properties form the basis of its widespread use in tissue engineering. Hyaluronan also forms a multivalent template for interactions with proteoglycans and other extracellular macromolecules that is important in the assembly of extracellular and pericellular matrices<sup>31</sup>. It is found in cartilage and synovial fluid where plays a critical dynamic role in both energy dissipation of fast compressive shock of the joint surface and control of fluid flow through the joint synovium<sup>32</sup>, connective tissue and vitreous humour<sup>31</sup>.

### 1.1.1.2 Chondroitin Sulfate Isomers (C4S, C6S, DS)

These GAGs are the most abundant in the human body, above all in the cartilaginous tissues, in the intervertebral disks, in the skin, tendons, in the cornea and aorta<sup>33</sup>. They are the only ones to contain the amino sugar galactosamine: the 4-sulphate (chondroitin A) and the 6-sulphate (chondroitin C) are homopolymers of disaccharides consisting of GlcA and GalNAc, which is esterified mainly in position 4 or 6 with sulphate groups. The number of repeated disaccharides varies according to the tissue with an average of 40 for chain. The DS (chondroitin B) shows a copolymeric nature containing both GlcA and IdoA. The two residues within each disaccharidic unit are linked by  $\beta$ (1,3) linkages, while the various units are united by  $\beta$ (1,4) linkages. Their ratio varies according on tissue type and also within the same tissue. The sulphation can be in

---

Antonio Cigliano, "Aortic and pulmonary bioprosthetic heart valves: an insight on glycosaminoglycan distribution and fine structure in decellularized porcine scaffolds for tissue engineering purposes" Dottorato in Biochimica, Biologia e Biotecnologie Molecolari – Università degli studi di Sassari.

position 4 or 6 in GalNac or in position 2 in IdoA or GlcA. The number of disaccharides repeated for chain is about 50-60.

#### ***1.1.1.3 Heparin (HE) and Heparan Sulfate (HS)***

These GAGs, like DS, are linear copolymers containing both GlcA and IdoA linked by  $\alpha(1,4)$  glycosidic linkage to GlcNac, while the various disaccharide units are linked by  $\beta(1,4)$  linkages. The two GAGs are distinguished by the size of the chains, the IdoA percentage and the number of sulfoester groups present in both hexuronic acid and hexosamine. IdoA prevails in HE, mainly O-sulfate in position 2; also the hexosamine is sulfated in position 4 or 6, and a fraction of the N-acetyl groups is replaced with N-sulfates. HE is distinguishable from HS by its high levels of such modifications. In heparin, approximately 80% of the disaccharide units are modified, while less than 10% of HS disaccharide units are epimerized or sulfated; HE is synthesized in mast-cells and plays a key role in the coagulation, while HS is synthesized by fibroblasts and endothelial cells and has been implicated in a wide variety of biological processes such as growth factor signaling, cell adhesion, wound healing, and tumor metastasis. HS is found on the surface of many cell types, in ECM of connective tissue, and in the basal membranes<sup>34</sup>.

#### ***1.1.1.4 Keratan Sulfate (KS)***

Disaccharidic unit of KS is characterized by a residue of D-galactose instead of hexuronic acid linked by  $\beta(1,4)$  linkage to GlcNac, while the disaccharidic units are linked by  $\beta(1,3)$  linkages. Both the residues of each units may contain a sulfate group in position 6. There are two classes of KS: type I (KSI), isolated from cornea where affects its transparency, is bound to protein core through a N-glycosidic link between GlcNac and a asparagine residue; Type II (KSII), isolated from cartilage, is bound to protein core by a O-glycosidic link between GlcNac and a Serine or Threonine residue<sup>16</sup>.

#### ***1.1.2 Proteoglycans (PGs)***

Proteoglycans (PGs) are proteins with long, unbranched polysaccharides chains (GAGs), ubiquitously expressed, and displaying a wide range of functions. After synthesis PGs are transported from the Golgi to their destinations: the extracellular matrix (ECM), the cell surface or intracellular organelles. Such vectorial transport requires mechanisms for recognition, sorting and delivery, which are especially important in cells, such as epithelial cells and neurons, where the cell membrane comprises separate domains. Recognition and sorting must require determinants in the GAG chains and/or in the PG protein cores<sup>16</sup>. Initially, PGs were grouped

---

Antonio Cigliano, "Aortic and pulmonary bioprosthetic heart valves: an insight on glycosaminoglycan distribution and fine structure in decellularized porcine scaffolds for tissue engineering purposes" Dottorato in Biochimica, Biologia e Biotecnologie Molecolari – Università degli studi di Sassari.

together because of the high negative charges of their GAG chains which make separation from other molecules by ion-exchange chromatography easy, and classified on the basis of the predominant type of GAG attached to the core proteins. However, PGs are not similar. The core protein size ranges from 10 kDa to > 500 kDa, and the number of GAG chains attached varies from one to >100. In addition, several PGs carry GAG chains of more than one type (hybrid PGs) and/or have additional N-linked or O-linked sugar modifications<sup>16</sup>. Furthermore, more recent comparisons of PG core protein structure by immunochemical and cloning methods have shown that these molecules exist as multigenic families, making a scaffold for GAG chains, and containing domains with particular biological activity<sup>4</sup>. PGs are placed in four main areas: 1) throughout the ECM, 2) associated with specialized structures of the ECM, such as basement membrane and basal laminae, 3) cell surface and 4) in intracellular structures, such as secretory storage granules and synaptic vesicles, suggesting that these molecules have numerous biological functions. GAG chains are large extended structures, with various alcoholic and acidic groups, and they dominate the physical properties of the protein to which they are attached. PGs in the ECM thus function physically as creators of a waterfilled compartment. Their high fixed negative charge attracts counter ions, and the osmotic imbalance caused by a local high concentration of ions draws water from the surrounding areas. Thus, PGs keep the matrix hydrated. A further physical property of the GAG chain is that they exclude other macromolecules while retaining permeability to low molecular weight solutes. The PGs thus create a water compartment, only part of which is available to other matrix macromolecules. This increases the concentration of the macromolecules and therefore may increase reaction rates promoting all interactions that are concentration dependent<sup>35-37</sup>. Although PGs constitute a minor component of vascular tissue, these molecules have been shown to influence a number of arterial properties such as visco-elasticity, permeability, lipid metabolism, hemostasis, and thrombosis<sup>33</sup>. The distribution of PGs throughout the blood vessel wall is variable and minimal variations in the GAG structure are responsible of the consistency of the existing several ECM (rigid, elastic and anelastic) determining its function. Versican/HA, Biglycan, Decorin, Perlecan, and Syndecan are the main PGs expressed in connective vascular tissue; content and distribution of these molecules is related to elderly and particular physiopathologic conditions<sup>47</sup>.

**VERSICAN** belongs to the family of hyaluronan-binding proteoglycans that include aggrecan, neurocan and brevican, constituting a gene family collectively termed 'hyalectins'. These PGs are components of the ECM and are found in a large number of tissues. Versican is a CS proteoglycan with a protein core of 263 kDa and binds 15-20 GAG chains, approximately. The gene and protein structure of versican follows a domain template. Successful cloning has

revealed the existence of at least four splice variants of versican, which differ in the size of the core protein and the number of glycosaminoglycan chains. The amino-terminal globular end (G1) binds to the hyaluronan, and the carboxy-terminal globular domain (G3) resembles the selectin family of proteins, consisting of a C-type lectin domain adjacent to two epidermal growth factor (EGF) domains and a complement regulatory region. The middle region of the versican core protein is encoded by two large exons that specify the CS attachment regions of versican<sup>38</sup>. Versican is present throughout the interstitial space of the vascular ECM and interacts with hyaluronan and link proteins to fill the ECM space not occupied by the fibrous components. These complexes create a reversibly compressible compartment and provide a swelling pressure within the ECM that is offset by the collagen fibrils<sup>4</sup>.

**BIGLYCAN** and **DECORIN** are small PGs that belong to the family of small leucine-rich proteins (SLRPs). These PGs contain an N-terminal domain that is usually substituted with either one (decorin) or two (biglycan) chondroitin/dermatan sulfate side chains, leading to pronounced polyanionic properties. The most salient feature of decorin and biglycan is the presence of 10 leucine-rich repeats (LRRs) flanked by cysteine-rich regions. Both biglycan and decorin are known to bind to different types of collagens<sup>39,40</sup>, their major functional roles include regulation of collagen fibrillogenesis, modulation of growth factor activity, and regulation of cellular growth. Decorin protein core (37 kDa) form a superhelix and is arranged so that the b-strands and a-helices are parallel to a common axis, thereby forming a horseshoe structure with the b-sheets lining the concave surface of the molecule and the a helices flanking the convex face. The concave surface can accommodate one triple helix of collagen type I and could account for the proposed binding sites and functional role of decorin in regulating collagen fibrillogenesis<sup>41,42</sup>. Biglycan protein core (38 kDa) was identified as a molecule that accumulates at the cell surface and in pericellular environments. Thus, based on its discrete cellular location, biglycan may have a different biological function in morphogenesis and differentiation<sup>36,43</sup>, and interact with several apoproteins<sup>44</sup>.

**PERLECAN** and **SYNDECAN** are PGs associated to basement and plasma membrane, respectively. Perlecan (470 kDa protein core) is a modular HSPG and is one of the largest single-chain polypeptides found in vertebrate and invertebrate animals. The various modules of perlecan and its HS chains take part in a large number of molecular interactions. Its binding partners include numerous heparin-binding growth factors such as fibroblast growth factor-2 (FGF2), vascular endothelial growth factor (VEGF) and platelet-derived growth factor (PDGF), and other proteins that are constituents of basement membrane or cell surfaces. Perlecan is also expressed in avascular tissues such as cartilage and various connective tissue stromas. So, it is

not surprising that perlecan is involved in a number of pathological processes, including atherosclerosis, angiogenesis and cancer<sup>45,46</sup>. The syndecans (31 kDa protein core) are a family of polymorphic cell surface proteoglycans bearing heparan sulfate and chondroitin sulfate chains. Their structure incorporates a short COOH terminal cytoplasmic domain, a transmembrane domain, and a large extracellular domain with numerous binding sites for GAG chains<sup>36</sup>. The cytoplasmic domain contains tyrosine residues that may provide phosphorylation sites for protein kinases, which are key enzymes in many signal transduction pathways, or may form sites for cross linkage with cytoskeletal elements. Syndecan interacts with growth factors, ECM receptors, coagulation enzymes, lipases, cytokines, fibronectin and collagen type I and II<sup>4</sup>.

### ***1.1.3 Collagens***

Collagens are proteins that consist of a triple helix of polypeptide chains, in which each chain contains at least one stretch of the repeating amino acid sequence Gly-X-Y. Six collagen types have been identified in blood vessels (I, III, IV, V, VI and VIII), of which type I and III comprise up to 80-90% of the total blood vessel wall<sup>48,49</sup>. Type I and III collagens are organized into distinct fibrillar bundles, either wedged between elastic fibers in elastic arteries or organized into nests surrounding medial arterial smooth muscle cells in muscular arteries<sup>50,51</sup>. These collagens provide tensile strength to the vascular wall. Type IV and VIII collagens are present within vascular basement membranes beneath endothelial cells and surrounding arterial smooth muscle cells. These molecules self-associate and interact with other molecules to form a supramolecular networks that serve as an anchoring substrates for vascular cells and as a permeability barrier to plasma proteins<sup>52</sup>. Type V and VI are present in small amounts in vascular tissue; the first codistributes with type I and may participate in the formation of collagen heteropolymers. A recent survey in human vascular tissue indicates its presence in thickened arterial intimas and in atherosclerotic fibrous plaques<sup>53</sup>. The second appears in all vascular layers between types I and III<sup>48,49</sup>; recent studies suggest that the type VI collagen fibril is bound with other ECM molecules, such as PGs, and may serve as an adhesive substrate for vascular cells<sup>54,55</sup>. The principal source of collagens biosynthesis is the smooth muscle cell; defects in the synthesis and deposition are associated to fibrous degenerative pathways such as atherosclerosis.

### ***1.1.4 Elastic fibers***

Another major component of blood vessels is the fibrous protein elastin, that provides mechanical strength and elasticity needed to accommodate pressure changes and hemodynamic changes due to pulsatile nature of blood flow. Elastic fibers are arranged into concentric sheets

or lamellae that separate different vascular layers. Frequently, the elastic lamellae are interconnected by radially oriented elastic fibers that facilitate the transfer of stress throughout the vessel wall<sup>50,51</sup>. The principal source of elastic fibers biosynthesis is the arterial smooth muscle cell that synthesizes it as a precursor molecule: tropoelastin.

## 1.2 Cardiac valves

### 1.2.1 Morphology

Cardiac valves are specialized forms of cardiovascular connective tissue designed to bear high mechanical stresses during the normal cardiac cycle. The valves show a complex architecture highly specialized, consisting of an avascular, semi-fluid and deformable matrix enriched in PGs, GAGs, collagen and elastic fibers. The four heart valves arise from embryonic mesenchymal outgrowths referred to as the endocardial cushions in a process termed valvuloseptal morphogenesis; two valves form in the atrioventricular canal (the tricuspid and mitral valves), with two valves forming in the ventricular outflow tract (aortic and pulmonary semilunar valves). It has been long accepted that all heart valves were simple structures whose contribution to the unidirectional flow of blood was merely passive movement in response to pressure gradients across the valve<sup>56</sup>. It is now clear that valves show several key characteristics as viability, sufficient strength to withstand repetitive and substantial mechanical stress, and ability to adapt and repair injury by connective tissue remodeling<sup>1</sup>. The four cardiac valves have microstructural similarities; however, the aortic valve best illustrates the essential features and serves as a paradigm for microstructural and cellular adaptation to functional requirements; furthermore, it is the most frequently diseased and also commonly transplanted. The semilunar valves are membranous sac-like flaps that show a sticking edge implanted on the fibrous ring placed on the border of the artery ostium and a free edge that protrudes in the vascular lumen. The aortic valve cusps undergo substantial changes in shape and dimension during the cardiac cycle. Microscopically, the aortic valve is composed of three distinct layers: (1) the *ventricularis* closest to the inflow surface, rich in elastin, (2) the *fibrosa* closest to the outflow surface, primarily composed of densely packed collagen, and (3) the centrally located *spongiosa*, largely composed of GAGs<sup>1-2</sup>. Together, collagen, elastin, and GAGs comprise the valvular ECM. Studies of normal, pathological, and substitute valves have demonstrated that the principal determinant of valve durability is the valvular ECM, whose quantity and quality depend on the viability and function of valvular interstitial cells (VICs)<sup>57</sup>. The principal cell types in the heart valve are the valvular interstitial cells (VICs) and valvular endocardial cells (VECs), smooth muscle, cardiac muscle and nerve cells<sup>2</sup>. VICs, believed to be responsible for maintenance of

---

Antonio Cigliano, "Aortic and pulmonary bioprosthetic heart valves: an insight on glycosaminoglycan distribution and fine structure in decellularized porcine scaffolds for tissue engineering purposes" Dottorato in Biochimica, Biologia e Biotecnologie Molecolari – Università degli studi di Sassari.



valvular structure, are numerous, elongated cells with many long, slender processes extending throughout the valve matrix. They connect to each other to establish a three-dimensional network throughout the entire valve, and are intimately associated with the valve matrix. It has been suggested that there may be two morphologically and structurally distinct populations of VICs: one possessing contractile properties, characterized by prominent stress fibers, and one possessing secretory properties, characterized by prominent rough endoplasmic reticulum (rER) and Golgi apparatus<sup>2</sup>. VICs are also the essential components of the intrinsic repair system of the valve. This regenerative process appears to be vital to normal valvular function and the absence of VICs in current prosthetic heart valve models is a probable factor contributing to structural failure<sup>2</sup>. The other major valve cell type is the VEC, which forms a functional envelope around each of the four heart valves. It seems reasonable that the VECs act to maintain a nonthrombogenic valve surface, similar to the vascular endothelium. Ultrastructurally, VECs have been shown to possess cell junctions, plasmalemmal vesicles and rER<sup>1,2</sup>. Forces acting on the valve at the macroscopic level such as pressure, shear stress, and tension, that during the cardiac cycle regulate the leaflet opening and closing and cause complex deformation of these structure, are translated into specific biomechanical responses at the tissue level, consisting in collagen uncrimping, reorientation, and fiber compaction, which are in turn transduced into a VIC response at the cellular level with intracellular signaling events leading to changes such as increased alpha smooth muscle actin ( $\alpha$ -SMA) expression, increased VIC stiffness, and increased ECM biosynthesis<sup>1,2</sup>. The pressure stresses are higher in the commissure and greater during the diastole regarding the systole. The entity of stresses in this area suggests that absence of continuous and rapid tissue turnover may lead to tissue usury and fatigue followed by its rupture<sup>58</sup>. Complex microstructural rearrangements and several specializations of collagen accommodate the cyclical pressure fluctuations during the cardiac cycle. Collagen fibers in a planar orientation in the fibrosa comprise the strongest portion of the leaflet that is responsible for bearing diastolic stress. GAGs in the spongiosa probably serve predominantly as a shock and shear absorber. The large cuspal deformation during the cycle between systole and diastole is facilitated by biomechanical cooperativity between collagen and elastin. Collagen fibrils are inelastic and incapable of supporting large strains; therefore, they have adaptations, macroscopic corrugations and microscopic crimp, that permit collagen stretching at minimal stress by unfolding. During valve opening, elastin stretches during extension of collagen crimp and corrugations. When the valve is closed, the collagen is fully unfolded and the load is shifted from elastin to collagen; elastin restores the contracted configuration of the cusp during systole<sup>1</sup>. GAGs are the major structural components of ground matrix found in connective valvular tissue.

---

Antonio Cigliano, "Aortic and pulmonary bioprosthetic heart valves: an insight on glycosaminoglycan distribution and fine structure in decellularized porcine scaffolds for tissue engineering purposes" Dottorato in Biochimica, Biologia e Biotecnologie Molecolari – Università degli studi di Sassari.

The nature and relative proportions of GAGs found in normal human valvular tissue and the changes occurring in these components as result of both their location, (aortic, mitral and tricuspidal valve) and aging have been described<sup>59</sup>. Occurrence of increased fibrosis, accompanied by calcification, degeneration of collagen fibers, and decrease in GAG content with age has also been demonstrated<sup>60</sup>. These changes were more prominent in aortic valve than in the others, with a GAG decrease of about 50% in the aortic valve, 25% in the mitral and 15% in the tricuspidal in men over 60 years old<sup>59</sup>. In normal human valves the major GAG components are HA (~ 60%), CS (~ 25/30%), and DS (~ 10/15%). Although GAG content is influenced by age, relative proportions of these three types of GAGs are not subjected to changes with aging<sup>59</sup>. Differently from the human, the porcine and bovine cardiac valves are mainly constituted of CS and DS<sup>61</sup>. Similarly to the human, the bovine aortic valves are richer in GAG content regarding those pulmonary and subject to a major decrease of the biosynthetic sulfate GAG activity with age<sup>62</sup>. The different GAG composition between these valves is probably associated to various pressure gradients or stresses to which they are subjected.

### ***1.2.2 Heart valve substitutes***

Valve replacement represents the most common surgical therapy for end-stage valvular heart disease<sup>63</sup>, and approximately 275,000 procedures are performed globally each year (Rabkin and Schoen, 2002). Exploration into heart valve replacement began in the 1950s, with the first successful human valve implantation being performed in 1952. Subsequent decades saw the development of numerous models of prosthetic heart valves with a progressive improving of design and manufacture technology; these remain the most common treatment for advanced heart valve disease<sup>64</sup>.

Originally, the optimal characteristics of the artificial heart valves were listed by Harken<sup>65</sup>:

- ✓ Not obstructive;
- ✓ Immediate and complete closure;
- ✓ Not thrombogenic;
- ✓ Infections resistant;
- ✓ Chemically inert and not hemolytic;
- ✓ Life span (years);
- ✓ Easy to insert in the appropriate physiological site.

In the reconstructive heart surgery, the bio-grafts may be either mechanical, consisting entirely of synthetic components, or obtained by biological tissue, bioprosthesis, distinguished in



allograft/homograft (human source) sterilized and cryopreserved, and xenograft (animal source) glutaraldehyde-fixed to reduce its immunogenicity and to stabilize it against the proteolytic degradation that would otherwise occur once implanted into the patient. Tissue crosslinks are formed by means of a number of complex reactions through which covalent bonds are created between the primary amine groups of proteins and the reactive aldehyde functionalities of glutaraldehyde (Glut). The result is a tightly crosslinked matrix of proteins, the majority of which is collagen. The leaflets maintain their flexibility, but there are structural modifications due to fixed non viable cells, and therefore incapable of a normal turnover and remodelling of the ECM components. The microstructure of the cusps, blocked in a phase of the cardiac cycle, show an alteration of the mechanical properties respect to the native cusps; at microscopic level, cuspal ECM components lacking free amine functionalities, such as elastin and GAGs, are not effectively stabilized, causing a loss of the endothelium, changes in spatial orientation of collagen and elastin fibers, decrease in GAG content and sovramolecular PG complex, rupture of plasma membrane and alteration of fibroblasts<sup>66,67</sup>. The major advantage of mechanical heart valves is their durability and longevity. However, the body's natural response to foreign materials can often result in thrombosis<sup>68</sup>, which can lead to mortality. For this reason, patients receiving mechanical heart valves are placed on long-term anticoagulation therapy<sup>69</sup>. Other limitations with mechanical valves are their association with infective endocarditis, risk of failure or separation of valvular components which may become embolised<sup>70</sup>. On the other hand, advantages of xenografts include an unlimited supply of donor tissue and superior hemodynamics with respect to mechanical valves; however, progressive tissue deterioration and calcification afflict biological replacements. Therefore, efforts of researchers are directed towards a better knowledge of heart valve structure and ECM component interactions that can significantly affect its life span. The main drawbacks of bioprosthetic heart valves (BHVs) are the following:

- ✚ Post implant cells are not viable;
- ✚ Collagen scaffold is chemically and mechanically altered;
- ✚ ECM does not repopulated;
- ✚ Cell debris facilitate calcification process.

In particular, numerous studies suggest that the maintenance of structural and functional ECM integrity is of primary importance for the performance of the valve substitutes. Depletions or alterations of the ECM components could be responsible for graft deterioration<sup>64</sup>. Over time, these bioprostheses become less extensible and progressively calcified, eventually leading to

structural deterioration, leaflet tears, and valve failure. Calcification and structural tear are synergistic processes affecting mainly the ECM during graft preparation. The principal changes described are: loss of endothelium and consequently loss of cohesion collagen fibers, mechanical damages due to fixation, absence of viable cells with consequent impossibility to renewing and remodeling the ECM. Moreover, because GAGs play an important role in maintaining tissue viscoelasticity, their loss from bioprosthetic valves might compromise mechanical function determining failure of valve integrity<sup>66,67,71-73</sup>. Several studies have been gathered on the improvement of fixation techniques; in fact, bioprostheses show an intrinsic calcification as consequence of the inability of the non viable cells to maintain a normal flow of intracellular  $\text{Ca}^{2+}$ . Calcific degeneration is often due to mechanical dysfunctions and vascular obstruction<sup>1,58</sup>. Moreover, the GLUT-fixation seems to enhance mineralization, indicating that calcific mechanism could depend from specific biochemical modifications induced by aldehydes at microstructural level<sup>66,74</sup>. The first  $\text{Ca}^{2+}$  storages are localized to the insertion areas of the cusps, the regions that are much more subjected to mechanical stresses<sup>58</sup>. The other cause of the valve grafts failure, in synergy with the calcification process, is the non-calcific structural degeneration due to the absence of physiological mechanisms of ECM self repairing. The factors involved in the ECM injuries are the anomalous movement of the valves, the inhibition of the structural rearrangement during the normal valve functioning, and the loss of the cell-mediated remodelling ability<sup>66</sup>. Molecular and biochemical alterations of collagen and elastin fibers and ECM degradation caused by the action of matrix metalloproteases (MMPs), collagenases, and high levels of  $\beta$ -glucuronidases could contribute to the progressive structural deterioration and calcification, suggesting that the tissue failure is related both to mechanical/calcific damages and to the action of proteolytic enzyme either intrinsic (immobilized tissue proteases derived by non viable cells) or extrinsic (infiltration of plasma components)<sup>66</sup>. On the other hand, GAGs because of the high concentration of negative charges and their inherent hydrophilicity are capable of absorbing a large amount of water within the tissue matrix. As a result, they are important components of the extracellular matrix of native heart valve cusps, especially with regards to mechanical behavior. It has been speculated that their ability to hydrate the spongiosa layer serves to decrease the shear stresses associated with cuspal flexure during valve function. In addition, the ability of this hydrated layer to absorb compressive forces may reduce buckling during flexion, which has been attributed to the mechanical failure of BHV cusps. Furthermore, the presence of negatively charged GAG molecules within the extracellular matrix of cuspal tissue may reduce calcification by chelating calcium ions, thereby preventing hydroxyapatite

nucleation. These observations suggest that the loss of GAGs may be an important factor in the structural and/or calcific failure of bioprosthetic heart valves<sup>67,75</sup>.

Regarding to homograft and allograft, sterilization and cryopreservation techniques are designed to obtain hydraulically functional valves with minimal cellular and tissue injuries. Cryopreservation induces damages to cellular level; in fact, it has been described an alteration of cytosolic and mitochondrial functionalities in endothelial cells<sup>76</sup> and fibroblasts<sup>77</sup>. The maintaining of cellular viability could be crucial in the restoration of those components of the ECM depleted or altered during tissue processing (ischemic interval, storage temperature, and the preservation modality)<sup>78</sup>. In particular, fibroblast viability is essential, because it play a key role in the turnover of the ECM components, in that sites subjected to elevated mechanical stresses<sup>58,79</sup>. To this aim, it is to emphasize that cellular viability in cryopreserved substitutes prepared by the standard protocols of Homograft Italian Bank, has been estimated between 80-90%<sup>77</sup>, although there is progressive loss of metabolic functioning in valve leaflet cells as storage times increase<sup>80</sup>. Homografts and allografts display a high hemodynamic profile, low incidence of thrombo-embolic complications, and infection resistance<sup>81</sup>. Current preservation techniques aim for a high degree of cellular viability at the time the graft is implanted. A previous research indicates that donor cells seem to disappear rapidly and will, in part, be replaced by host cells<sup>80</sup>. Furthermore, it is known that cryopreserved valves are capable of evoking cellular and humoral immune responses in vitro and in vivo. It is uncertain, however, whether the immunogenicity of these valves contributes to the loss of valve cellularity and structure and thereby to their dysfunction and failure<sup>80</sup>. The failure of this type of grafts is to ascribe to the insufficient ability to cell growing, repairing, and remodelling, causing the progressive tissue deterioration associated to calcium phosphate storages in correspondence of the regions subjected to high mechanical stresses (commissures) including ECM injury, collagen type I damages, and loss and/or modifications of GAGs<sup>82-85</sup>. However, although the choice of homograft/allograft is better than xenograft or mechanical prostheses their insufficient availability has always limited the use<sup>64</sup>.

Several studies are focusing on the potential applications of tissue engineering (TE) in regenerative medicine that range from structural tissue to complex organs. Essentially, TE consist in the development of a scaffold, a biocompatible and biodegradable decellularized structure, seeded with cells to obtain a new, functional tissue. The scaffold should temporarily supply as biomechanical support until the seeded cells produce a new ECM, and it depends by the ability to the seeded cells to renew, to repair and to remodel themselves recreating a structure similar to the native<sup>64</sup>. A widely accepted paradigm of tissue engineering comprises [1] a

---

Antonio Cigliano, "Aortic and pulmonary bioprosthetic heart valves: an insight on glycosaminoglycan distribution and fine structure in decellularized porcine scaffolds for tissue engineering purposes" Dottorato in Biochimica, Biologia e Biotecnologie Molecolari – Università degli studi di Sassari.

scaffold, that is pre-seeded with [2] cells, followed by [3] an in-vitro stage of tissue formation typically conducted in a bioreactor, that recapitulates a physiological metabolic and mechanical environment, and subsequently, following implantation of the construct, [4] an in-vivo stage of tissue growth and remodeling. The key pathophysiological processes occurring during the in-vitro and in-vivo phases are cell proliferation and migration, ECM production and organization, scaffold degradation, and tissue remodeling. The in-vivo but not the in-vitro phase can involve recruitment of the recipient's inflammatory cells. The resulting tissue engineered construct will likely contain some combination of seeded and/or recipient-derived new cells.

An alternative pathway utilizes an unseeded scaffold that incorporates biological "information" designed to attract and direct the formation of circulating endogenous precursor cells, potentially both endothelial and mesenchymal, in-vivo. Moreover, host inflammatory cells may play a role in the in-vivo phase of either approach<sup>1</sup>.

Scaffolds can be obtained from biodegradable synthetic polymer and/or natural allograft or xenograft decellularized tissues. Both types show advantages and disadvantages: synthetic scaffolds allow to control material structure and properties like pore size, stability, degradation rate, and they are easily reproduced; however, they are resorbable and present difficulty in controlling cell adhesion and tissue reorganization, inflammation due to incomplete polymer degradation or lack of biocompatibility, space formerly occupied by polymer and its interstices is replaced by fibrosis that limits perfusion to deep cells. Natural scaffolds maintain architecture of the native tissue and biological information (reactive sites, growth factors), but they are potentially resorbable, decellularization may alter physical properties, difficulty of cell penetration into interior, may induce immunologic reaction and potential for calcification<sup>1</sup>. Potential cellular sources for seeding of scaffolds to fabricate heart valves include differentiated tissue-specific cells such as allogenic or xenogenic endothelial cells and/or fibroblasts<sup>86,87</sup>, autogenic smooth muscle cells, interstitial cells and fibroblasts<sup>88</sup>, and stem cells that may be autologous or allogenic avoiding the problem of cell phenotype preselection<sup>88</sup>. Following extensive studies using ovine vascular derived cells and regarding future human application the suitability of human cells derived from various human cell sources have been investigated. Among the most promising are vascular-derived cells, bone marrow-derived cells, blood-derived cells, umbilical cord-derived cells and chorionic villi-derived cells, particularly for pediatric application<sup>89</sup>. Seeded cells can then use the body's natural structural cues to promote organization, growth and development of the replacement 'tissue'. The scaffolds are designed to degrade or hydrolyze in vivo as the implanted cells produce and organize their own ECM network.

---

Antonio Cigliano, "Aortic and pulmonary bioprosthetic heart valves: an insight on glycosaminoglycan distribution and fine structure in decellularized porcine scaffolds for tissue engineering purposes" Dottorato in Biochimica, Biologia e Biotecnologie Molecolari – Università degli studi di Sassari.

However, successful tissue regeneration may not always be achieved ‘simply’ by combining cells and scaffolds. The gene expression of cells and tissue formation can be regulated or promoted by the addition of growth factors, cytokines or hormones<sup>2,86,90</sup>. The mechanisms of valve morphogenesis, during the embryonic development, are complex and highly regulated, therefore it could be difficult to stimulate all the mechanisms involved in the regulatory pathway<sup>64</sup>. With this approach it is possible to obtain a viable and autologous TE that can be implanted promoting the development of cardiac valves mimicking growth, repair and remodel such as native tissue. Inherent studies are needed regarding the progressive evolution of this structures, the gene expression and the functionality of the viable cells, the composition and organization of the new ECM, the effect due to the mechanical deformation of the ECM on the cellular increase, cell-cell and cell-matrix interactions.

Although, TE constitute the ideal substitute as it arranges nearly all the characteristics of a native valve, we are still far to obtain adequate outcomes for the implant in the man. Meantime, parallel studies are trying to improve the quality of bioprostheses and mechanical prostheses performing their hemodynamic characteristics and limiting the calcific/non calcific injuries due to deterioration of the substitutes, with the intent to increase the graft durability and to reduce the necessity of repetitive surgeries.

## 2. Aim of this work

GAGs are heterogenous polysaccharides not only for the type of constituent disaccharidic unit but above all for their molecular size, charge density, sulfation pattern, and epimerization degree<sup>12,15</sup>. With the exception of hyaluronan, GAGs are usually linked to a protein core forming PGs. PGs are implied in numerous biological processes and the majority of these functions is mediated by the structural characteristics of their GAG chains. The structural analysis of GAGs implies the characterization of disaccharide components, whose features determine the bioactivity of the molecules. The structural analysis of GAGs consist in chemical or enzymatic depolymerization, followed by separation and characterization of the products by electrophoretic (Capillary Zonal Electrophoreses CZE, Fluorophore Assisted Carbohydrate Electrophoresis FACE)<sup>91-93</sup> or chromatographic (HPLC) techniques<sup>94</sup>. PGs are essential components of the ECM, playing structural and functional key roles in the valve tissue; in fact, they are differently distributed in the cardiac valves and their turnover is higher at commissure level, where mechanical stresses are maximal<sup>4</sup>. Qualitative and quantitative modifications of these molecules due to GAG structural modifications and/or altered rates of turnover can be associated to several pathological diseases. Since GAGs/PGs influence the abilities of cell population to grow onto acellular scaffold (bioprosthesis) or cryopreserved grafts (homograft), the study of their content and composition in cardiac valves could reveal key factors in tissue engineering and development of valve bioprostheses.

In a recent publication, cryopreservation has been reported to determine a marked loss of cellular viability and tissue integrity. Moreover, a relevant GAG content depletion, with possible consequences on the graft performance<sup>64</sup>, and the presence of low-sulfate chondroitin sulfate<sup>83,84</sup> have been observed. A loss of GAGs has been also described in the fixed tissue during the preparation of bioprostheses, probably affecting the potentiality of repopulation of these devices. While a limited number of reports have described the intact valve GAGs, little attention has been made to the complex valve microstructure and GAG fine structure, i.e. the relative abundance of variously sulfated disaccharides. Sulfation patterns of GAG chains are thought to be critical for GAG function and cellular signaling<sup>109</sup>. Reports characterizing valve GAGs are even fewer and largely regard bioprosthetic valves and tissue engineering heart valves (TEHVs).

The aim of this study was to characterize the composition as well as the fine structure of GAGs in native and decellularized porcine aortic and pulmonary valves to assess eventual GAG compositional changes during development of a scaffold for TEHVs. Therefore, we have compared GAG content, composition, and structure in control fresh valves (NT) and in valves subjected to a decellularization treatment (TRICOL) depicted to completely eliminate the

---

Antonio Cigliano, "Aortic and pulmonary bioprosthetic heart valves: an insight on glycosaminoglycan distribution and fine structure in decellularized porcine scaffolds for tissue engineering purposes" Dottorato in Biochimica, Biologia e Biotecnologie Molecolari – Università degli studi di Sassari.

cellular components maximizing the maintenance of the endothelial basal membrane, the ECM structural network and its integrity, the interactions of small PGs with collagen fibrils, and the mechanical properties of the valve<sup>95,96,110</sup>. The fine structural analysis of GAGs from different valve regions was performed by means of fluorophore-assisted carbohydrate electrophoresis (FACE).

Finally, the objective is to obtain a scaffold suitable to the cellular repopulation and to get useful informations for the improvement of the graft preparation procedures. Detailed structural GAG analysis is appeared irrenounceable for the reason that selective depletions and/or modifications of GAGs following decellularization processing could influence preparation of the biological valve substitutes, their ability to recellularization, ECM remodelling and renewal, their resistance to calcification, structural deterioration, and non-thrombogenic nature.

This work was conducted in collaboration with the researchers of Biomedical Experimental Sciences Department, University of Padua.



### 3. Materials and methods

#### 3.1 Tissue analysis

Porcine hearts from 10-12 month old pigs with weights ranging from 160 to 180 kg were obtained from a local slaughterhouse. Within 2 hours from death valve conduits were harvested and decellularized by a detergent-based procedure. We have analyzed 24 semilunar porcine valves divided in 2 groups: 12 aortic and 12 pulmonary valves; for each group 6 samples were considered as control and referred to as NT and 6 samples decellularized and referred to as TRICOL. All tissue sampling and decellularization steps were conducted by our colleagues in Padua. Briefly, NT samples were rinsed in isotonic saline solution and immediately processed. TRICOL samples were extracted for 10 h with 1% (w/v) Triton X-100 in presence of protease inhibitors (PI). After further 10 h extraction without PI and washing overnight in 0.1% (w/v) Triton X-100, samples were extracted at 4°C for two 10-h periods in PBS containing 0.5M NaCl. Following hypotonic PBS washing, Triton X-100 was replaced by 10 mM sodium cholate, and extraction resumed for two 10-h periods at room temperature. All samples were finally washed in 10% (v/v) isopropanol, saline, equilibrated in water and wet weight recorded. All extraction procedures were carried out in presence of NaN<sub>3</sub> 0.1% in fully degassed solution containing 10 mM sodium ascorbate and under N<sub>2</sub> atmosphere. Tissue processing for the GAG analysis is delivered in the flow diagram in **Fig. 1**.

Three zones were cut using a surgical blade and separately processed: the aortic root wall, the commissure, and the leaflet. After peeling and segregation of the three different types of tissue, their wet weight was measured. Tissues were fixed with 20 volumes of acetone at 4°C for 24 h, delipidated with 20 volumes of chloroform:methanol (2:1, vol/vol) at 4°C for 24 h, and, after centrifugation at 3300 x g for 15 minutes, dried at 60°C. The final weight (dry defatted tissue [DDT] weight) of the artery wall, commissure, and the leaflet was recorded.

#### 3.2 Extraction and purification of total GAGs

DDTs (100 mg) were rehydrated for 24 h at 4°C in 0.1 M sodium acetate, pH 6.0, containing 5 mM cysteine and 5 mM ethylenediaminetetraacetic acid (37 volumes for gram of DDT). Papain (0.3 U/mg of DDT) was then added to the mixture, which was incubated at 56°C for 24 h under mild agitation. The digest was clarified by centrifugation (9000 × g for 20 min at +4°C). Digest supernatant was loaded on a (diethylamino)ethyl-cellulose column (0.7 × 6 cm, 2.3 mL), equilibrated with 50 mM sodium acetate, pH 6.0. The column was then washed with 50 mL of the same buffer and eluted with a two-step salt gradient (IE 0.55 and IIE 1.0 M NaCl). Fractions



of 1 mL were collected. These were assayed for hexuronate content by the method of Bitter and Muir, using glucuronolactone as a standard<sup>97</sup>. Fractions containing GAGs were pooled and precipitated using 4 volumes of cold absolute ethanol. The mixture was left overnight at -20°C and the precipitate was separated by centrifugation, washed twice with ethanol, and then dried.

### 3.3 Acetate cellulose electrophoresis

GAG composition was determined by discontinuous electrophoresis according to Cappelletti et al.<sup>98</sup>. This method, combined with the differential susceptibility of GAGs to precipitation by solvents, allows optimal and rapid separation of intact GAGs with high resolution and sensitivity (10 ng detection limit). GAGs were separated in 0,25 M barium acetate buffer, pH 5.0 by three steps. Titan III-H zone cellulose acetate plate (6.0 x 7.5 cm, Helena BioSciences) was first dipped in distilled H<sub>2</sub>O to a height of about 1.5 cm; the sheet was immediately blotted between filter papers. The opposite end was then immersed in 0.1 M barium acetate, pH 5.0 for 5.5 cm, leaving a narrow band (2 – 4 mm large) apparently dry between H<sub>2</sub>O and buffer. This band will disappear during the run. The sheet was blotted again between the filter papers, and 5 µl sample were applied in the narrow dry band. The loaded sheet was subjected to 5 mA constant current for about 6 minutes and then soaked in 0.1 M barium acetate, pH 5.0 for 2 minutes. In the next step, a 15 mA constant current was applied for 14 minutes. The sheet was again removed from the chamber and immersed for 2 minutes in a similar buffer containing 15% (v/v) ethanol. A subsequent electrophoretic step was carried out at 12 mA constant current for 17 minutes. After the electrophoresis the sheet was stained in 0.1% (w/v) Alcian Blue solution for 10 minutes, and destained in 1% (v/v) acetic acid.

GAGs identification was performed treating aliquots of the samples with specific eliminases, as previously described<sup>99</sup>. The specificity and the efficiency of enzyme treatments were checked on standard GAGs under the same experimental conditions. Based on their decreasing electrophoretic mobility, standard GAGs run in the following order: chondroitin sulfate (C4S/C6S), dermatan sulfate, hyaluronan, heparan sulfate and slow dermatan sulfate. The relative percentage of each band per lane was determined by densitometry scanning of Alcian Blue stained strips and analyzed with a software. Before the scanning the plate was immersed in a solution containing 71% (v/v) methanol, 25% (v/v) acetic acid and 4% (v/v) clear acid to a better acquisition of the bands.

### 3.4 GAG depolymerization

The enzymes that are mainly used for the degradation of the CS isomers or galactosaminoglycans (GalAGs), belong to the family of chondro/dermato lyases. All of them act on the  $\beta(1\rightarrow4)$  bond between hexosamine and uronic acid and produce disaccharides possessing a double bond between C-4 and C-5 of the uronic acid. The unsaturated uronic acid strongly absorbs ultraviolet light at 232 nm ( $E=5500 \text{ M}^{-1} \text{ cm}^{-1}$ ) and this wavelength is used for the quantitation of the products. Chondroitinase ABC, from *Proteus Vulgaris*, degrades hyaluronan (HA), and all chondroitin sulfate isomers (CS A, CS C, and DS), producing disaccharide units containing  $\alpha,\beta$ -unsaturated uronic acids:  $\Delta\text{Di-0S}_{\text{HA}}$ ,  $\Delta\text{Di-0S}_{\text{CS}}$ ,  $\Delta\text{Di-mono4S}$ ,  $\Delta\text{Di-mono6S}$ . This enzyme is not active regarding heparin, heparan sulfate and keratan sulfate. Chondroitinase AC II, from *Arthrobacter Aurescens*, acts on the same bond, but it is not able to degrade DS, whereas chondroitinase B degrades only DS. A combination of enzymes may also be used for the characterization of these GAGs in a biologic sample. Treatment of GalAGs with chondroitinase AC II, which completely degrades the CS chains and, to some extent, the DS ones, revealed that almost 36% of DS was not degraded by chondroitinase AC II<sup>100</sup>.

Dried GAGs were resuspended in 100  $\mu\text{L}$  of 0.1 M ammonium acetate, pH 8.0<sup>101</sup>. Digestion with chondroitinase ABC and chondroitinase AC II was performed at 37 °C for 24 h, using 0.1 U/100  $\mu\text{g}$  uronic acid. The digestion mixture was boiled for 1 min to inactivate the enzyme, centrifuged at  $11,000 \times g$  for 5 min, and dried. Then, aliquots were taken for derivatization and FACE analysis.

### 3.5 Fluorotagging with 2-Aminoacridone (AMAC)

The free reducing groups that are exposed by enzyme cleavage, can be derivatized with 2-aminoacridone by reductive amination in the presence of sodium cyanoborohydride ( $\text{NaBH}_3\text{CN}$ ) as described by Calabro et al<sup>102</sup> (**Fig. 3.1**). Particularly, a 40  $\mu\text{L}$  volume of 12.5 mM AMAC solution in glacial acetic acid/DMSO (3:17 v/v) was added to the lyophilized sample aliquots, and samples were incubated for 10–15 minutes at room temperature. Then 40  $\mu\text{L}$  of 1.25 M  $\text{NaBH}_3\text{CN}$  in ultrapure water were added to each sample and then mixtures were incubated at 45°C for 4 hours. After derivatization, 20  $\mu\text{L}$  of glycerol (20% final concentration) were added to each sample prior to electrophoresis. If necessary, samples were diluted with buffer containing 6% glacial acetic acid, 20% glycerol, 34% DMSO, and 480 mM  $\text{NaBH}_3\text{CN}$ <sup>103</sup>.

### 3.6 FACE analysis

PAGE was performed according to Karousou et al.<sup>104</sup>, in a MiniProtean II cell vertical slab gel electrophoresis apparatus (Bio-Rad). Briefly, the resolving gel consisted of 25%T/3.75%C polyacrylamide in a 187.5 mM Tris-borate and 187.5 mM Tris-HCl buffer, pH 8.8. The stacking gel was 5%T/1.5%C in 0.36 M Tris-HCl buffer, pH 8.8. A 5  $\mu$ L volume of each sample was loaded in each well; a marker sample containing bromophenol blue was also run in a well with no sample. Electrophoresis was performed in 0.15 M Tris-borate, pH 8.8, at 400 V and 4 °C and terminated when the marker dye was 1.2 mm from the bottom of the gel. Gels were scanned in a UV-light box using a CCD camera (Gel Doc XR System) and analyzed with Quantity One 4.6.3 from BioRad Laboratories.

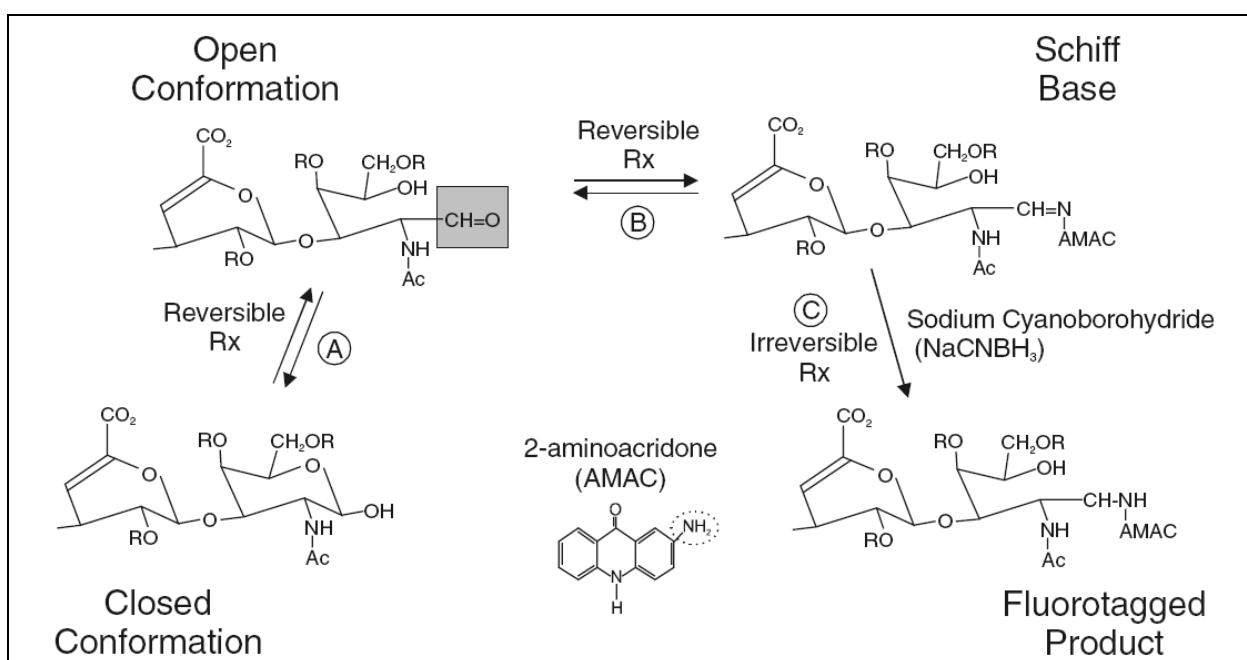


**Fig. 3.1** - Reducing sugars in solution are in equilibrium (A) between a six-member closed pyranose ring conformation and an open conformation containing a free reducing aldehyde (shaded box). The amine group (dashed circle) of 2-aminoacridone (AMAC) reacts with the free reducing aldehyde to form a Schiff base (B) that is stabilized by reduction with cyanoborohydride (C). The final AMAC-tagged saccharide yields a fluorescent signal dependent solely on the fluorotag, not the chemistry of the saccharide. The Rs indicate locations, which may be occupied with either a sulfate group or a proton.

### 3.7 CS calibration curve and statistical analysis

For quantification of  $\Delta$ -disaccharide from CS isomers, a CS calibration curve was build using commercial chondroitin sulfate A submitted to chondroitin ABC and AC lyase treatment and

derivatization procedure. Data are reported as mean  $\pm$  standard deviation or total numbers and relative frequencies. For comparison between two groups, Student's t-test was performed. A value of  $P \leq 0.05$  was considered statistically significant. The analyses were performed with Microsoft SPSS 11.0 and SigmaStat 3.11.0 software.

#### 4. Results and Discussion

Two main groups of porcine heart valves were analyzed for GAGs determination: aortic valves (n = 12) and pulmonary valves (n = 12). For each group, analysis was carried out on six native control (NT) and six decellularized samples (TRICOL). From each valve conduit three zones were processed: the arterial wall, the commissure or sinus and the leaflet (**Fig. 2**).

In **Table I** total GAG contents, expressed as  $\mu\text{g}$  hexuronate/mg DDT, are reported. In both valves the three selected areas were significantly different in GAG content<sup>83</sup> GAG concentration increases moving from the artery wall towards the leaflet. In decellularized aortic valve GAG content was significantly reduced in both commissure and leaflet, whereas in pulmonary valves the treatment significantly affected only the leaflet. Moreover, the determination of total GAG content in native valves indicated higher levels in aortic commissures and leaflets compared to the same areas from pulmonary valves.

Tissue extracted GAGs were freed from proteins and purified by ionic exchange chromatography in two steps with different ionic strength (IE and IIE). Typical electrophoresis patterns obtained from low and high charge fractions in control and TRICOL samples are shown in **Fig. 3**. Low charge fractions consist of four bands corresponding in order of migration to CS<sub>slow</sub>, DS HA, HS; the high charge fractions show only two bands corresponding to CS and DS. For each band the identification was assessed by observing its disappearance following specific enzymatic cleavage. GAGs distribution in the three examined areas in both valve conduits is reported in **Fig. 4**.

In both control valve conduits the leaflets exhibited the highest GAG concentration (see **Table I**), that decreased in commissures and even more in artery walls. GAG analysis indicated that deep structural dissimilarities in polysaccharide chains exist depending on their topographic localization. In particular, the higher GAG total concentration in sinuses and leaflets is associated to higher relative contents of HA and CS<sub>slow</sub>.

So, respect to the artery wall, in valves we found a reduced content of heteropolymeric GAGs, presenting higher epimerization and sulfation degree and therefore with a greater capability to interact with other ECM components, in favour of homopolymeric GAGs, that probably have a structural role. Moreover, a slow moving CS isomers seems to be valve tissue-specific.

GAG levels in aortic root were significantly depleted after decellularization by TRICOL treatment. Interestingly, in pulmonary root only the leaflet was significantly affected by the treatment. GAG distribution in each native control area was similar for aortic and pulmonary roots. Decellularization of native aortic valve induced a massive loss of GAGs from each area without changing their relative proportions, indicating that the loss was not selective. On the

---

Antonio Cigliano, "Aortic and pulmonary bioprosthetic heart valves: an insight on glycosaminoglycan distribution and fine structure in decellularized porcine scaffolds for tissue engineering purposes" Dottorato in Biochimica, Biologia e Biotecnologie Molecolari – Università degli studi di Sassari.

contrary, decellularization of the pulmonary valve, that greatly affected GAG content of leaflet, also produced a deep change in the GAG distribution, suggesting a selective extraction of HA and in minor amount of CS, as confirmed by the reduction in CS/DS ratio.

The concept of decellularization or tissue engineering of heart valves was developed and modified by several groups in the course of years. It is believed that the process of decellularization can reduce or eliminate the immune response or calcific degeneration associated with non autologous cells and cell membranes, thereby increasing implant durability<sup>105</sup>. Nevertheless, decellularization results in a depletion of the spongiosa layer. It has been suggested that the principle function of the spongiosa is to dampen the vibrations in the fibrosa associated with leaflet flexion during closure. Due to the loss of major GAG component in the spongiosa, associated to changes in mechanical and structural properties of decellularized leaflets, disruption of the ECM, early tissue degradation, and calcification may result, affecting on the durability of the leaflets<sup>106</sup>.

The bulk of GAGs in native valve is represented by HA and CS isomers, comprising a slow migrating CS. Since the relative proportion of HS in commissures and leaflets of both native valves is very little (less than 7%), we focalized on the fine structural characterization of CS isomers. The abundance of particular GAGs and PGs can vary according to different biological needs of the tissues. For example, the dermatan sulfate (mostly 4-sulfated) PGs decorin and biglycan regulate the formation and orientation of collagen fibrils and hence tissue tensile strength, whereas the hyaluronan (HA), which is not covalently bound to a core protein, entraps large amounts of water to create a swelling force<sup>107</sup>. It has been speculated that their ability to hydrate the spongiosa layer serves to decrease the shear stresses associated with cuspal flexure during valve function. In addition, the ability of this hydrated layer to absorb compressive forces may reduce buckling during flexion. Furthermore, it has been previously speculated that the presence of negatively charged GAG molecules within the extracellular matrix of cuspal tissue may reduce calcification by chelating calcium ions, thereby preventing hydroxyapatite nucleation<sup>66,67,108</sup>. Taken together, these observations suggest that the loss of GAGs may be crucial for the development of new bioprostheses and tissue engineering.

GAGs obtained from the three examined areas have been structurally characterized, after ABC and AC chondroitinase treatment, by polyacrilamide gel electrophoresis of their constituent  $\Delta$ -disaccharides marked with the fluorophore 2-aminoacridone (AMAC). Recent developments in carbohydrate analysis using FACE<sup>102</sup>, have enabled the study of GAGs in heart valves using novel and efficient methods. This new technology can quickly provide characteristics about the GAG profile, chain lengths, and sulfation patterns that can provide clues to the identity of

---

Antonio Cigliano, "Aortic and pulmonary bioprosthetic heart valves: an insight on glycosaminoglycan distribution and fine structure in decellularized porcine scaffolds for tissue engineering purposes" Dottorato in Biochimica, Biologia e Biotecnologie Molecolari – Università degli studi di Sassari.

particular PGs within valve tissues and might be used to postulate their mechanical contributions to valve function. In fact FACE is a high sensitivity and resolution method; AMAC is a fluorescent molecule with  $\lambda_{exc} = 425$  and  $\lambda_{em} 520$  nm that may be monitored both by UV and LIF detection. The derivatization procedure is relatively simple and fast, the derivatization efficiency is elevated, and the stability of adduct is satisfactory. Moreover, the excess of derivatizing reagent does not interfere with the separation. In **Fig. 5** typical patterns of derivatized  $\Delta$ -disaccharides are shown. FACE analyses allow us to detect both mono- and di-sulfate CS disaccharides, also discriminating between the non-sulfated forms released from CS isomers and those released from HA. In this study, the designation of a GAG as containing iduronate or glucuronate was based on the susceptibility to chondroitinase AC II treatment.

The distributions of  $\Delta$ -disaccharides from low (A,C) and high (B,D) charge GAGs in each selected area (**Fig. 6**) are similar for control and decellularized valves. Moreover, they did not differ in aortic and pulmonary conduits. In **Fig. 7** the TRICOL-induced depletions for both total and single  $\Delta$ -disaccharides content (expressed as  $\mu\text{g}$  of hexuronate per mg of DDT) are shown. The percentages reported near TRICOL bars point out the relative loss for each  $\Delta$ -disaccharide following decellularization procedure, confirming a marked but not selective GAG extraction for aortic valve and a lesser extraction, affecting mainly HA, for pulmonary valve.

**Fig. 8** shows the epimerization pattern in both valves for CS isomers in the three examined areas. These analyses rely on the knowledge that chondroitinase AC II does not cleave IdoA clusters. Native and TRICOL valves, either aortic or pulmonary, did not exhibit significant differences in iduronation degree, confirming that CS isomers extraction is not selective (see fig. 7).

In **Table 2** total epimerization patterns for native and TRICOL-treated aortic and pulmonary valves are compared. There was no significant difference between control and decellularized valves, although it is remarkable that pulmonary valve present a higher iduronation degree than aortic conduit.

**Table 3** exhibites  $\Delta\text{di-mono6S}/\Delta\text{di-mono4S}$  ratio in both valves. In aortic leaflet this ratio was significantly reduced after treatment, mostly reflecting CS isomers sulfation from the low charge fraction. No significant difference in  $\Delta\text{di-mono6S}/\Delta\text{di-mono4S}$  ratio was detected after treatment of pulmonary conduit. However, by comparing the two types of native valves, significant differences were exhibited for low charge GAG fraction from leaflet and arterial wall. In **Table 4** data for CS isomers sulfation degree are reported. TRICOL-treatment does not produce significant modifications in total GAG sulfation degree, although it displays some effects on low charge GAG fraction from aortic sinus and leaflet. Interestingly, significant differences in the

sulfation degree were detected between native aortic and pulmonary valve conduit, regarding high charge GAGs.

In conclusion, results on GAG structural characterization in native and decellularized valves suggest that the depletion in total content may also produce changes in GAG distribution. Since the structural properties of galactosaminoglycan, such as the extent and pattern of sulfation, the charge density, and the isoform of the uronic acid moiety on the GlcA are implicated in their bioactivity, their selective modifications could affect the chances of a scaffold for tissue engineering. In vivo each of them can be modulated, mediating several biological processes that promote the interaction with different molecules. Sulfation pattern is critical for the determination of the biological actions of GAGs. Sulfation is also critical for the ionic interaction between GalAGs and other molecules. The 5-position carboxylic acid group of GluA is synthesized in the glucuronic acid isoform of a chondroitin sulfate galactosaminoglycan but is subject to isomerisation, generating the iduronic acid derivative and thus the dermatan sulfate galactosaminoglycan. These isomers display different levels of structural flexibility and potentially different ionic charge distributions. Compared to the glucuronic acid isoform, the iduronic acid form provides a more rigid structure<sup>75</sup>.



## 5. Conclusions

The goal of heart valve tissue engineering is to regenerate a functional structure containing endothelial and interstitial cells capable of continuously remodeling the ECM that functions structurally and biomechanically as a valve leaflet. Furthermore, it could be used to repair congenital defects in children, because bioprostheses have no ability to grow, and therefore require more than two replacements, increasing operative risks. Despite an exciting potential for tissue engineered heart valves, many unanswered questions remain and significant technical barriers must be overcome before widespread clinical application can be envisioned.

This study shows that, there is a profound loss of GAGs during decellularization procedure. The reason for these losses is likely the molecular structure of the proteoglycans that contain these GAGs. Distribution of PGs and GAGs in vascular tissue is complex, district- and layer-specific, associated with different mechanical environments, and could have important implications for heart valve tissue engineering. Although some of these compositional differences may appear quite subtle, such as the presence and location of sulfation on GAG chains, these fine structural distinctions may have important biological roles such as serving as binding sites for other matrix components or for signaling cell differentiation. It is thought that decellularization treatment extracts easily hyaluronan and chondroitin/dermatan-6-sulfate, which are those that exist in tissues as part of the aggregate of hyaluronan and the proteoglycan versican. Unlike versican, core protein of decorin, largely chondroitin/dermatan-4-sulfate, is located adjacent to collagen fibrils and could be less susceptible to selective extraction<sup>73</sup>.

Although the biosynthetic pathways of CS isomers are known, the mechanisms that regulate their post-translational modifications are far to be clear. These post-synthetic events determine the huge heterogeneity of GAGs. It is evident that in valvular tissue, GAG metabolism is unusual; low sulfation of some CS could be due to lack of sulfation group donors (PAPS) and therefore limiting regard to quick turnover. GAG synthesis in this tissues deserves further studies, particularly the functional role of low sulfated GAGs, sulfation patterns in general, and epimerization degree. The possibility to assess carefully the  $\Delta$ di-mono4S and  $\Delta$ di-mono6S content in tissues is important because the ratio of these disaccharides changes during aging and could be used as a marker of matrix aging<sup>101</sup>. Moreover, modifications of the  $\Delta$ di-mono6S/ $\Delta$ di-mono4S ratio are thought to play a critical role in diseases<sup>102</sup>. Furthermore, this ratio might be used to hypothesize the type of PGs found in the valves associated to GAG class concentrations and fine structure characteristics<sup>101</sup>.

Future studies are need to examine the inherent complexity within valve tissues, due to the histological layers, mechanical forces, matrix composition and effects of aging, and also the

---

Antonio Cigliano, "Aortic and pulmonary bioprosthetic heart valves: an insight on glycosaminoglycan distribution and fine structure in decellularized porcine scaffolds for tissue engineering purposes" Dottorato in Biochimica, Biologia e Biotecnologie Molecolari – Università degli studi di Sassari.

functional characteristic of different GAGs that could have impact on the function of normal valves and on the choice of the candidate valve to produce the best scaffold for the development of a tissue engineering heart valve.

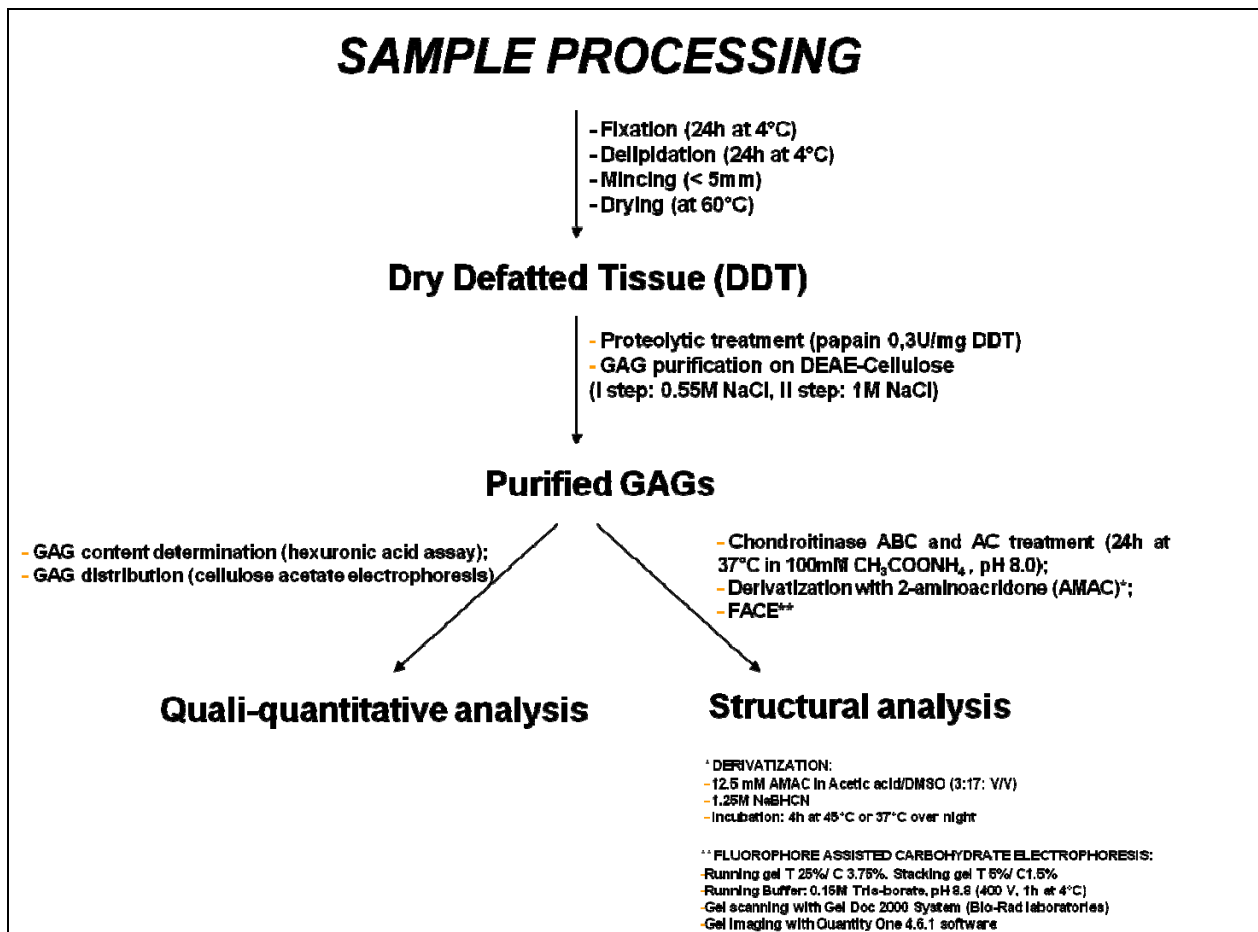


Fig. 1 – Flow diagram showing tissue processing for GAG analysis.

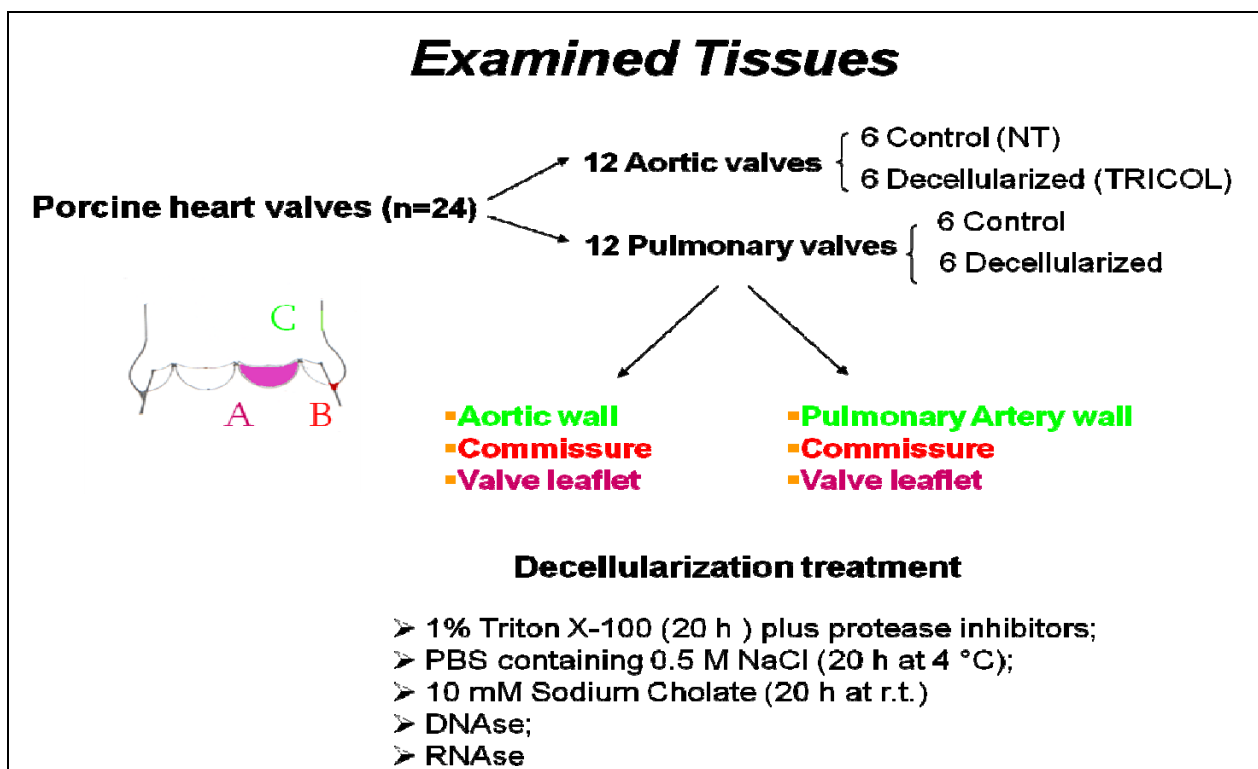


Fig. 2 – Examined tissues.

**Table 1** - Total GAG content ( $\mu\text{g}$  hexuronate/mg DDT) in the selected areas (artery wall, sinus, and leaflet) of both valves. *t*-Test is referred to Control vs Decellularized samples and Pulmonary vs Aortic valve.

		<i>Aortic root</i>		<i>p value</i>
		Control	Decellularized	<i>Control vs Decellularized</i>
Artery root wall		5.49 $\pm$ 0.59	4.28 $\pm$ 1.04	<b>0.033</b>
Commissure		12.99 $\pm$ 4.04	10.48 $\pm$ 1.96	<b>0.004</b>
Leaflet		16.69 $\pm$ 1.64	8.94 $\pm$ 1.19	<b>2.93 E-06</b>
		<i>Pulmonary root</i>		<i>p value</i>
		Control	Decellularized	<i>Control vs Decellularized</i>
Artery root wall		5.72 $\pm$ 0.91	5.10 $\pm$ 0.71	0.22
Commissure		6.98 $\pm$ 0.53	5.51 $\pm$ 2.38	0.17
Leaflet		10.44 $\pm$ 1.73	6.60 $\pm$ 2.55	<b>0.012</b>
<i>Pulmonary vs Aortic</i>		<i>p value</i>		
		Control	Decellularized	
Artery root wall		0.54	0.16	
Commissure		<b>0.004</b>	<b>0.012</b>	
Leaflet		<b>0.001</b>	0.14	



**Fig. 3** – GAG patterns in low (IE) and high (IIE) charge fractions of NT and TRICOL samples, assessed by cellulose acetate electrophoresis.

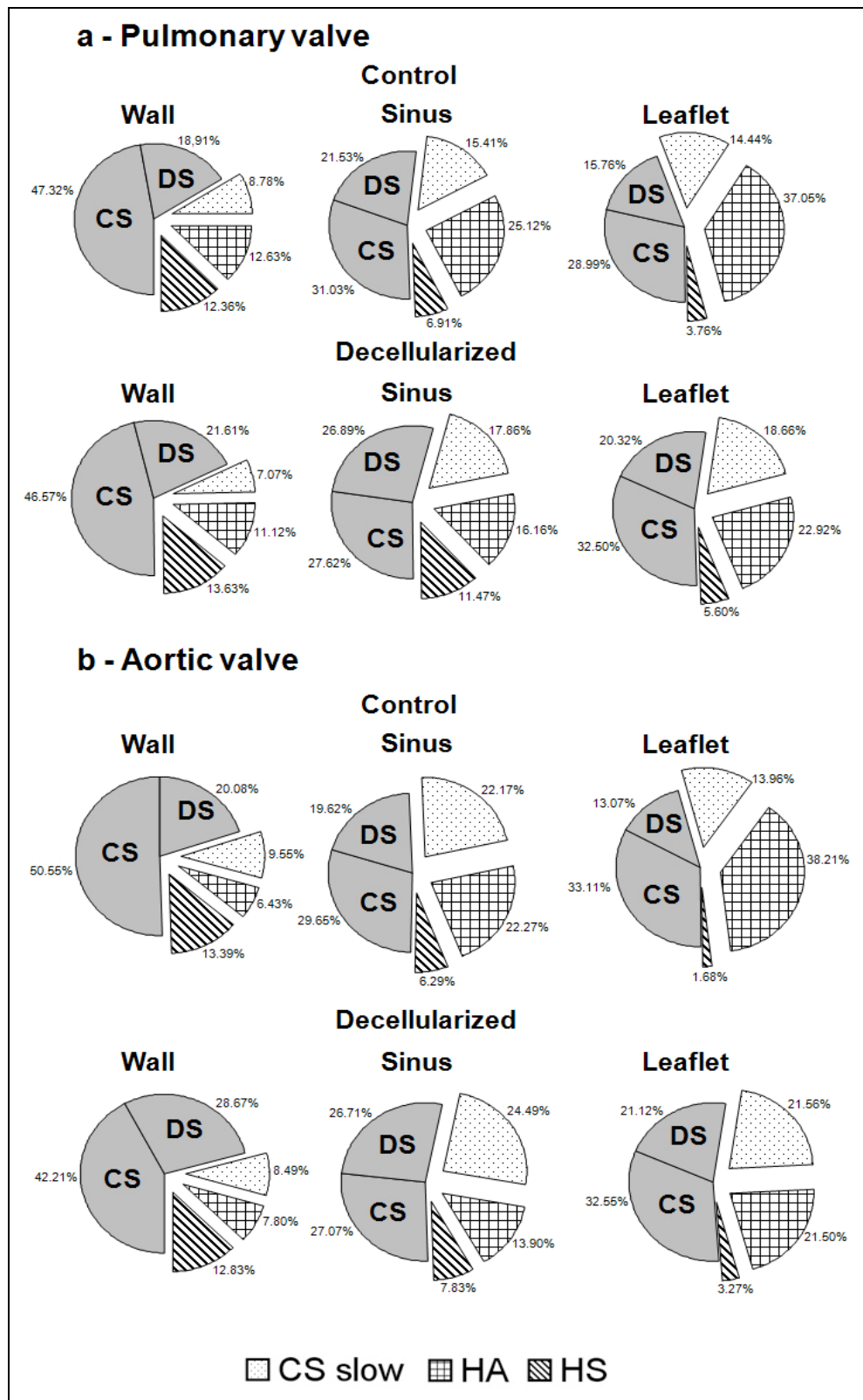


**Fig. 4** – GAG distribution in the examined areas of aortic and pulmonary valve conduit. The percentages are calculated as sum of GAG distribution in low and high charge fractions.

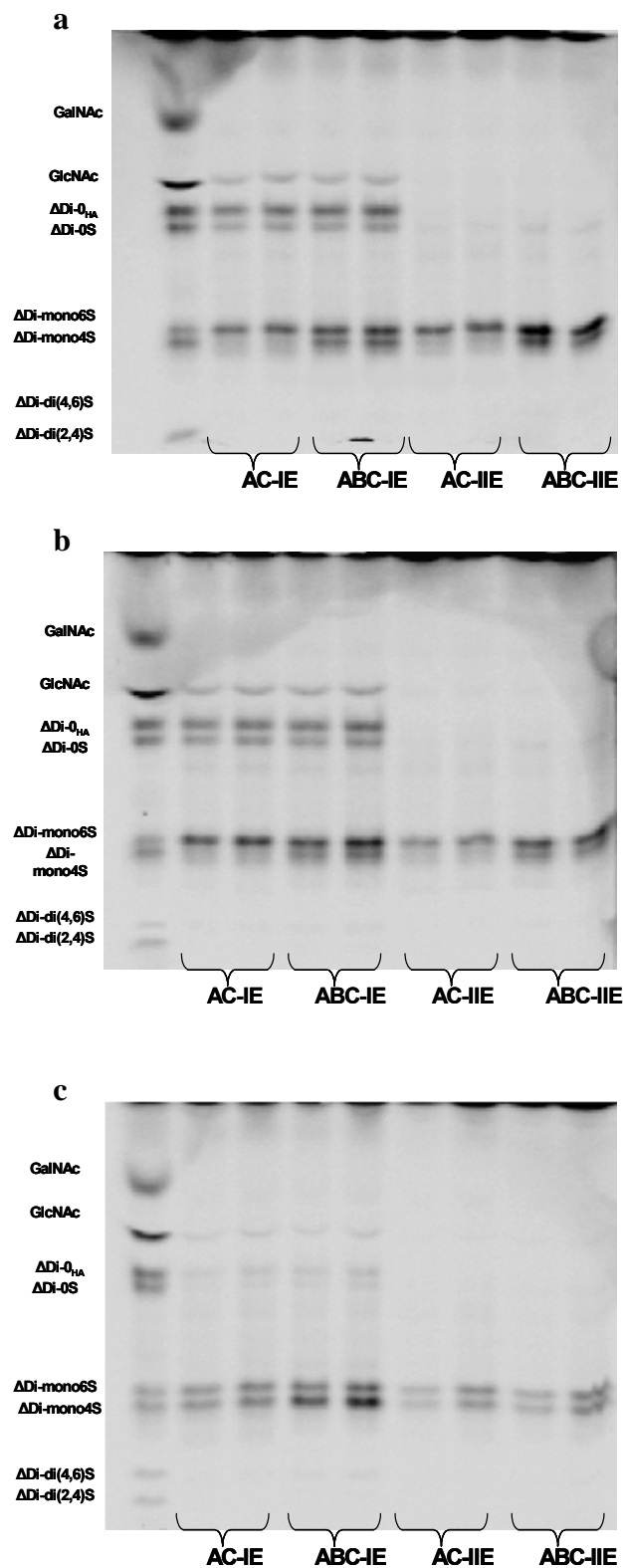


**Fig. 5** –FACE separation of unsaturated AMAC-labeled disaccharides patterns obtained from low (IE) and high charged (IIE) GAGs after depolymerization with Chase ABC and AC. Representative patterns for leaflet (panel a), sinus (panel b), and artery wall (panel c) of native aortic valve are reported (inverted images). Electrophoresis was performed in 0.15 M Tris borate, pH 8.8, at 400 V and 4 °C for 1 h approximately.

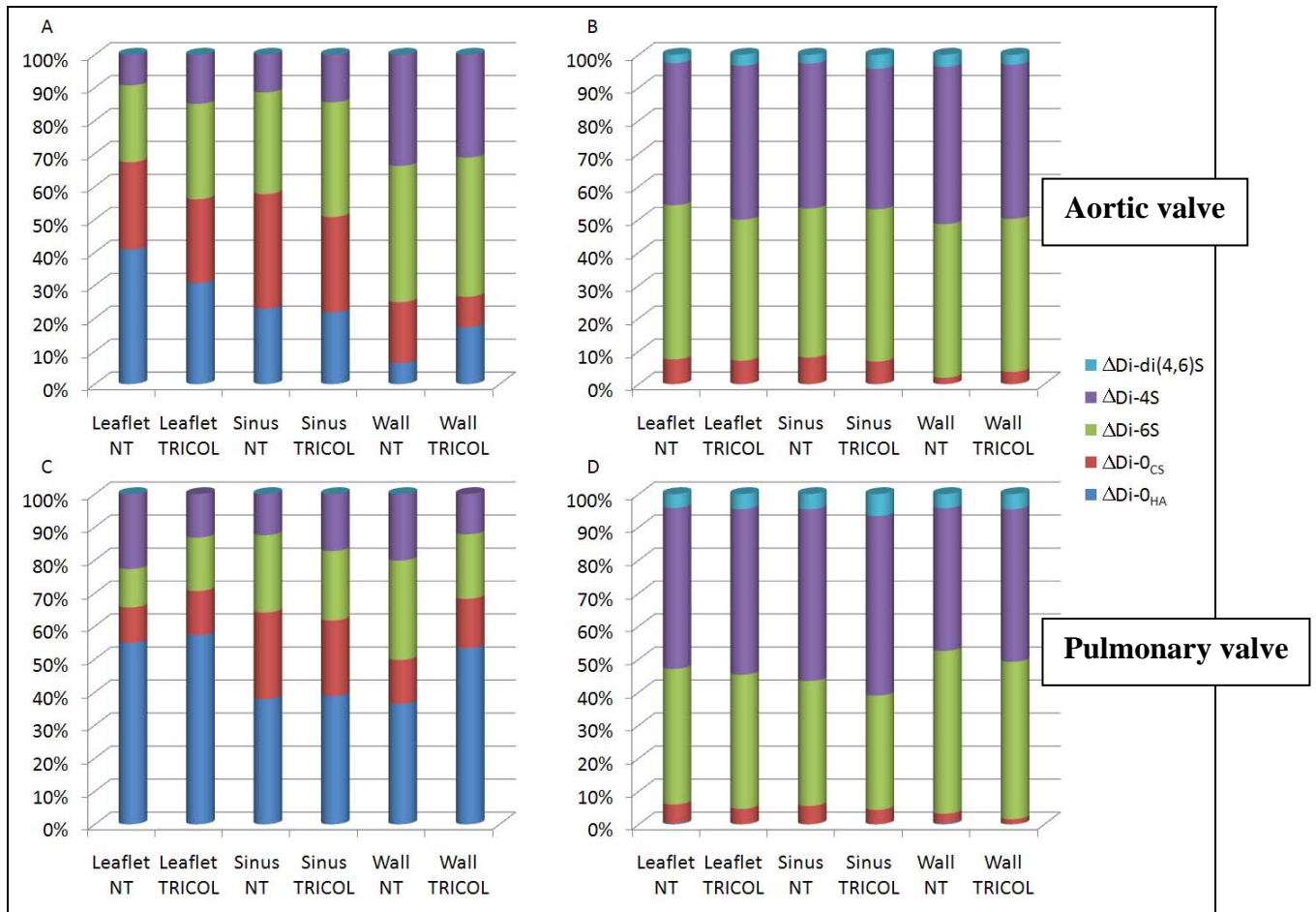


**Fig. 6** – Relative  $\Delta$ -disaccharides content in low (A and C) and high (B and D) charge GAGs in the three native and decellularized examined areas.

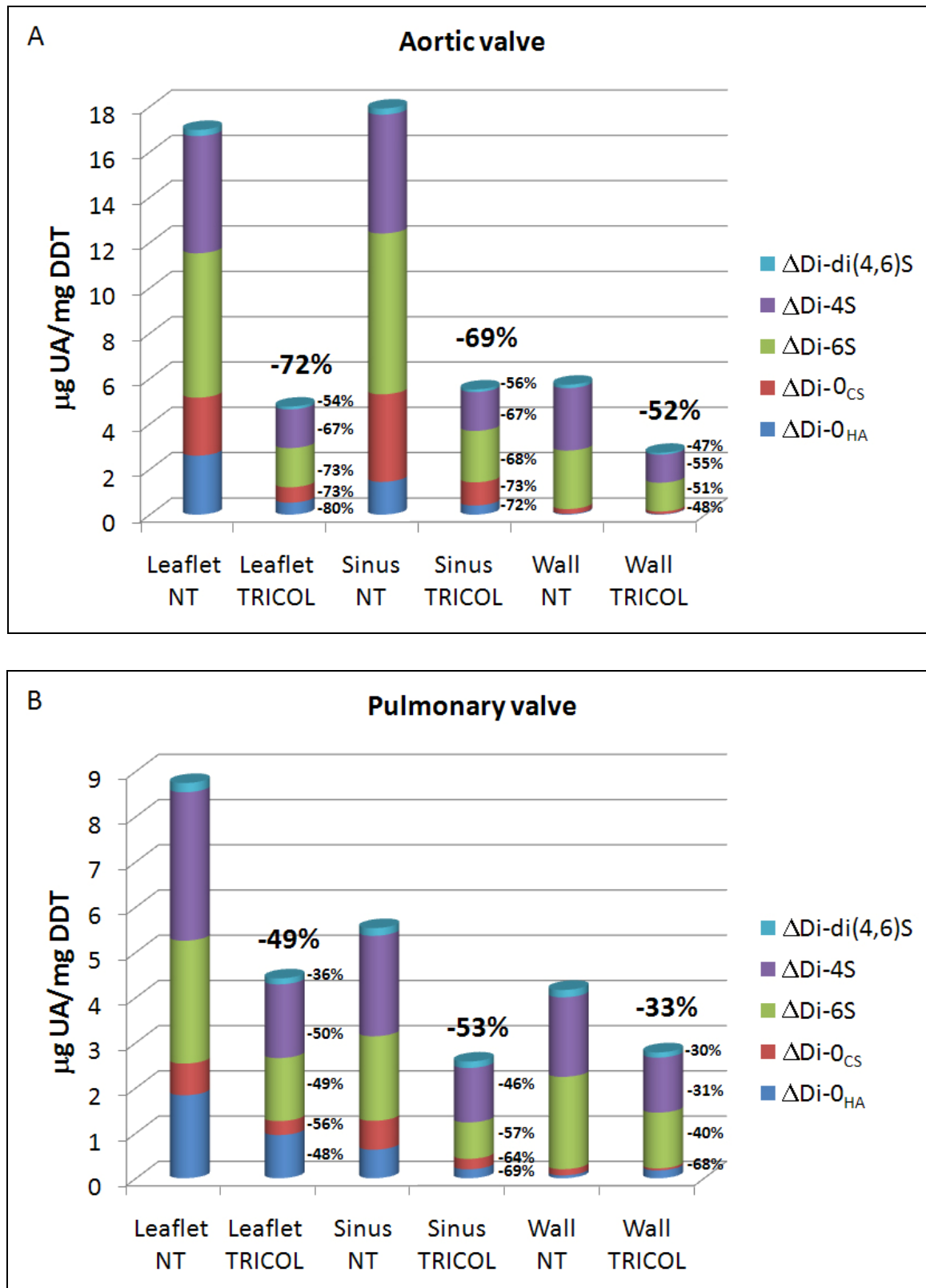


**Fig. 7** – Total  $\Delta$ -disaccharides content in aortic (A) and pulmonary (B) valves in the three examined areas. The percentages in decellularized sample bars are referred to total and single loss of  $\Delta$ -disaccharides following the treatment.



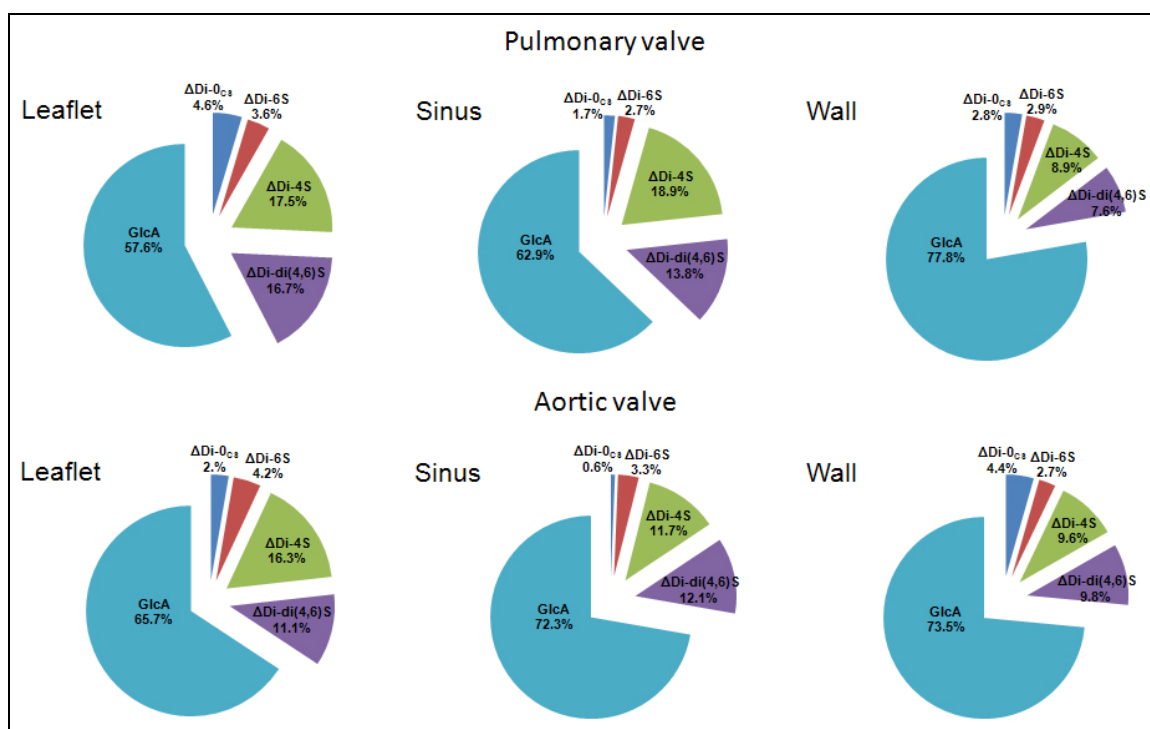


**Fig. 8** – Representative outline of the epimerization pattern in the selected areas of both valves. The percentages are reported as mean values obtained from native and decellularized valves.

**Table 2** – Total epimerization pattern in the three examined areas of both valves (values are means  $\pm$  standard deviation).

% IdoA	AORTIC VALVE		PULMONARY VALVE	
	NT	TRICOL	NT	TRICOL
LEAFLET	36.45 $\pm$ 12.69	32.06 $\pm$ 12.84	48.37 $\pm$ 10.90	36.39 $\pm$ 17.72
SINUS	24.96 $\pm$ 6.66	30.52 $\pm$ 5.24	37.58 $\pm$ 11.02	36.61 $\pm$ 8.31
ARTERY WALL	22.06 $\pm$ 6.67	30.91 $\pm$ 13.79	27.08 $\pm$ 3.14	17.34 $\pm$ 12.15

**Table 3** – CS isomers sulfation pattern in the three examined areas of both valves (values are means  $\pm$  standard deviation). Significant differences are reported in bold

AORTIC VALVE						
	$\Delta$ di-mono6S/ $\Delta$ di-mono4S IE		$\Delta$ di-mono6S/ $\Delta$ di-mono4S IIE		$\Delta$ di-mono6S/ $\Delta$ di-mono4S	
	NT	TRICOL	NT	TRICOL	NT	TRICOL
LEAFLET	3.57 $\pm$ 0.47	2.48 $\pm$ 0.39	2.97 $\pm$ 0.29	2.55 $\pm$ 0.38	3.07 $\pm$ 0.26	2.54 $\pm$ 0.30
SINUS	3.36 $\pm$ 0.50	2.67 $\pm$ 0.61	2.32 $\pm$ 0.35	2.41 $\pm$ 0.82	2.62 $\pm$ 0.23	2.56 $\pm$ 0.66
ARTERY WALL	1.86 $\pm$ 0.25	1.27 $\pm$ 0.49	1.56 $\pm$ 0.26	1.73 $\pm$ 0.22	1.58 $\pm$ 0.23	1.75 $\pm$ 0.22
<i>t</i> -test Control vs Decellularized						
LEAFLET	0.012		0.13		0.036	
SINUS	0.129		0.84		0.874	
ARTERY WALL	0.075		0.361		0.313	
PULMONARY VALVE						
	$\Delta$ di-mono6S/ $\Delta$ di-mono4S IE		$\Delta$ di-mono6S/ $\Delta$ di-mono4S IIE		$\Delta$ di-mono6S/ $\Delta$ di-mono4S	
	NT	TRICOL	NT	TRICOL	NT	TRICOL
LEAFLET	1.41 $\pm$ 1.63	2.36 $\pm$ 1.04	2.64 $\pm$ 0.50	2.41 $\pm$ 0.36	2.66 $\pm$ 0.39	2.40 $\pm$ 0.46
SINUS	1.97 $\pm$ 1.32	2.05 $\pm$ 0.63	2.34 $\pm$ 0.21	2.02 $\pm$ 0.43	2.53 $\pm$ 0.16	2.01 $\pm$ 0.45
ARTERY WALL	1.45 $\pm$ 0.25	1.13 $\pm$ 0.88	1.57 $\pm$ 0.18	1.47 $\pm$ 0.23	1.57 $\pm$ 0.18	1.49 $\pm$ 0.26
<i>t</i> -test Control vs Decellularized						
LEAFLET	0.364		0.49		0.423	
SINUS	0.926		0.227		0.073	
ARTERY WALL	0.514		0.533		0.632	
AORTIC VALVE NT vs PULMONARY VALVE NT						
	$\Delta$ di-mono6S/ $\Delta$ di-mono4S IE		$\Delta$ di-mono6S/ $\Delta$ di-mono4S IIE		$\Delta$ di-mono6S/ $\Delta$ di-mono4S	
LEAFLET	0.044		0.294		0.129	
SINUS	0.097		0.919		0.527	
ARTERY WALL	0.058		0.979		0.953	

**Table 4** – Total sulfation degree in the three examined areas of both valves (values are means  $\pm$  standard deviation). Significant differences are reported in bold.

AORTIC VALVE						
	$\Delta$ Di-Sulfated/ $\Delta$ Di-Unsulfated IE		$\Delta$ Di-Sulfated/ $\Delta$ Di-Unsulfated IIE		$\Delta$ Di-Sulfated/ $\Delta$ Di-Unsulfated	
	NT	TRICOL	NT	TRICOL	NT	TRICOL
LEAFLET	1.23 $\pm$ 0.09	1.73 $\pm$ 0.23	12.38 $\pm$ 1.27	14.42 $\pm$ 5.62	5.43 $\pm$ 1.17	6.15 $\pm$ 1.46
SINUS	1.21 $\pm$ 0.24	1.76 $\pm$ 0.32	11.46 $\pm$ 1.20	13.86 $\pm$ 2.64	3.76 $\pm$ 0.22	4.93 $\pm$ 2.32
ARTERY WALL	6.21 $\pm$ 6.07	4.61 $\pm$ 3.95	52.16 $\pm$ 10.70	44.97 $\pm$ 28.79	40.12 $\pm$ 17.40	43.99 $\pm$ 30.03
<i>t</i> -test Control vs Decellularized						
LEAFLET	0.007		0.505		0.472	
SINUS	0.033		0.149		0.354	
ARTERY WALL	0.674		0.656		0.831	
PULMONARY VALVE						
	$\Delta$ Di-Sulfated/ $\Delta$ Di-Unsulfated IE		$\Delta$ Di-Sulfated/ $\Delta$ Di-Unsulfated IIE		$\Delta$ Di-Sulfated/ $\Delta$ Di-Unsulfated	
	NT	TRICOL	NT	TRICOL	NT	TRICOL
LEAFLET	2.98 $\pm$ 2.11	2.12 $\pm$ 0.48	16.90 $\pm$ 2.91	22.68 $\pm$ 9.67	10.91 $\pm$ 3.52	10.39 $\pm$ 1.21
SINUS	1.38 $\pm$ 0.30	1.80 $\pm$ 0.62	17.64 $\pm$ 3.86	22.53 $\pm$ 5.29	6.49 $\pm$ 1.07	10.56 $\pm$ 5.79
ARTERY WALL	4.41 $\pm$ 1.45	1.23 $\pm$ 2.12	41.54 $\pm$ 18.21	64.31 $\pm$ 12.37	43.50 $\pm$ 21.70	62.49 $\pm$ 24.60
<i>t</i> -test Control vs Decellularized						
LEAFLET	0.459		0.296		0.786	
SINUS	0.273		0.186		0.216	
ARTERY WALL	0.048		0.084		0.291	
AORTIC VALVE NT vs PULMONARY VALVE NT						
	$\Delta$ Di-Sulfated/ $\Delta$ Di-Unsulfated IE		$\Delta$ Di-Sulfated/ $\Delta$ Di-Unsulfated IIE		$\Delta$ Di-Sulfated/ $\Delta$ Di-Unsulfated	
LEAFLET	0.148		0.03		0.025	
SINUS	0.415		0.022		0.002	
ARTERY WALL	0.584		0.353		0.816	

1. Mendelson K and Schoen FJ - **Heart valve tissue engineering: concepts, approaches, progress, and challenges**. *Annals of Biomedical Engineering* 2006, 34(12):1799-1819
2. Flanagan TC and Pandit A - **Living artificial heart valve alternatives: a review**. *European Cells and Materials* 2003, Vol 6:28-45
3. Kleinman HK, Philp D, Hoffman MP - **Role of the extracellular matrix in morphogenesis**. *Current Opinion in Biotechnology* 2003, 14:526–532
4. Wight TN - **Atherosclerosis and coronary artery disease**. Lippincott-Raven Publisher, Philadelphia 1996, 421-440
5. Streuli C - **Extracellular matrix remodelling and cellular differentiation**. *Current Opinion in Cell Biology* 1999, 11:634-640
6. Aumailley M, Gayraud B - **Structure and biological activity of the extracellular matrix**. *J Mol Med* 1998, 76:253-265
7. Ingber DE - **Mechanical signaling and the cellular response to extracellular matrix in angiogenesis and cardiovascular physiology**. *Circ Res* 2002, 91:877-887
8. Daniel OT, Abrahamson D - **Endothelial signal integration in vascular assembly**. *Ann Rev Physiol* 2000, 62:649-671
9. Stupack DG, Cheresh DA - **ECM remodeling regulates angiogenesis: endothelial integrins look for new ligands**. *Sci STKE* 2002, 2002:PE7
10. Davis GE, Bayless KJ, Mavil A - **Molecular basis of endothelial cell morphogenesis in three-dimensional extracellular matrices**. *Anat Rec* 2002, 268:252-275
11. Raman R, Sasisekharan V, Sasisekharan R - **Structural insights into biological roles of protein-glycosaminoglycan interactions**. *Chemistry & Biology* 2005, 12:267–277
12. Gama CI, Hsieh-Wilson LC - **Chemical approaches to deciphering the glycosaminoglycan code**. *Current Opinion in Chemical Biology* 2005, 9:609–619
13. Monzon ME, Casalino-Matsuda SM, Forteza RM – **Identification of glycosaminoglycans in human airway secretions**. *Am J Respir Cell Mol Biol* 2006, 34:135–141
14. Kolset SO, Prydz K, Pejler G – **Intracellular proteoglycans**. *Biochem J* 2004, 379:217-227
15. Sugahara KY, Mikami T, Uyama T, Mizuguchi S, Nomura K, Kitagawa H - **Recent advances in the structural biology of chondroitin sulfate and dermatan sulfate**. *Current Opinion in Structural Biology* 2003, 13:612–620
16. Prydz K and Dalen KT - **Synthesis and sorting of proteoglycans**. *Journal of Cell Science*, 2000; 113:193-205

17. Sugahara K, Kitagawa H - **Heparin and eparan sulfate biosynthesis**. IUBMB Life 2002, 54:163–175
18. Bradbury EJ, Moon L, Popat RJ, King VR, Bennett GS, Patel PN, Fawcett JW, McMahon SB - **Chondroitinase ABC promotes functional recovery after spinal cord injury**. Nature 2002, 416:636–640
19. Perrimon N, Bernfield M - **Specificities of heparan sulphate proteoglycans in developmental processes**. Nature 2000, 404:725–728
20. Mizuguchi S, Uyama T, Kitagawa H, Nomura KH, Dejima K, Gengyo-Ando K, Mitani S, Sugahara K, Nomura K - **Chondroitin proteoglycans are involved in cell division of Caenorhabditis elegans**. Nature 2003, 423:443–448
21. Kleene R, Schachner M - **Glycans and neural cell interactions**. Nat Rev Neurosci 2004, 5:195-208
22. Lin X - **Functions of heparan sulfate proteoglycans in cell signaling during development**. Development 2004, 131:6009–6021
23. Casu B, Guerrini M, Guglieri S, Naggi A, Perez M, Torri G, Cassinelli G, Ribatti D, Carminati P, Giannini G, et al. - **Undersulfated and glycol-split heparins endowed with antiangiogenic activity**. J Med Chem 2004, 47:838–848
24. Livanainen E, Kahari VM, Heino J, Elenius K - **Endothelial cell-matrix interactions**. Microsc Res Tech 2003, 60:13-22
25. Schachter H, Chen S, Zhang W, Spence AM, Zhu S, Callahan JW, Mahuran DJ, Fan X, Bagshaw RD, She YM et al. - **Functional posttranslational proteomics approach to study the role of N-glycans in the development of Caenorhabditis elegans**. Biochem Soc Symp 2002, 69:1-21
26. Sasisekharan R, Shriver Z, Venkataraman G, Narayana-sami U - **Roles of heparan-sulphate glycosaminoglycans in cancer**. Nat Rev Cancer 2002, 2:521–528
27. Liu D, Shriver Z, Venkataraman G, El Shabrawi Y, Sasi-sekharan R - **Tumor cell surface heparan sulfate as cryptic promoters or inhibitors of tumor growth and metastasis**. Proc Natl Acad Sci USA 2002, 99:568–573
28. Cossart P, Sansonetti PJ - **Bacterial invasion: the paradigms of enteroinvasive pathogens**. Science 2004, 304:242-248
29. Piwnica-Worms D, Schuster DP, Garbow JR - **Molecular imaging of host-pathogen interactions in intact small animals**. Cell Microbiol 2004, 6:319-331
30. Day AJ, de la Motte CA – **Hyaluronan cross-linking: a protective mechanism in inflammation?** TRENDS in Immunology 2005, 26(12):637-643
31. Toole BP - **Hyaluronan: from extracellular glue to pericellular cue**. Nature 2004, 4:528-539

32. Day AJ, Sheehan JK - **Hyaluronan: polysaccharide chaos to protein organisation.** Current Opinion in Structural Biology 2001, 11:617–622
33. Wight TN - **Cell biology of arterial proteoglycan.** Arteriosclerosis, 1989; 9:1-20
34. Nakato H, Kimata K – **Heparan sulfate fine structure and specificity of proteoglycan functions.** Biochim Biophys Acta 2002, 1573:312-318
35. Poole AR – **Proteoglycans in health and disease: structures and functions.** Biochem J 1986, 236:1-14
36. Hardingham TE, Fosang AJ – **Proteoglycan: many forms and many function.** FASEB J 1992, 6:861-870
37. Wight TN, Kinsella MG, Potter-Perigo S, Riddi A – **Extracellular matrix: structure and function.** New York 1985, Alan Liss:331-332
38. Wight TN - **Versican: a versatile extracellular matrix proteoglycan in cell biology.** Current Opinion in Cell Biology 2002, 14:617–623
39. Tufvesson E, Westergren-Thorsson G - **Biglycan and decorin induce morphological and cytoskeletal changes involving signalling by the small GTPases RhoA and Rac1 resulting in lung fibroblast migration.** Journal of Cell Science 2003, 116:4857-4864
40. Iozzo RV - **The biology of the small Leucine-rich Proteoglycans: functional network of interactive proteins.** J Biol Chem 1999, 274[27]:18843-18846
41. Weibert IT, Harrison RW, Iozzo RV – **Model structure of decorin and implications for collagen fibrillogenesis.** J Biol Chem 1996, 271(50):31767-31770
42. Scott JE – **Proteodermatan and proteokeratan sulfate (decorin, lumican/fibromodulin) proteins are Horseshoe shaped. Implications for their interaction with collagen.** Biochemistry 1996, 35[27]:8795-8799
43. Iozzo RV, Murdoch AD – **Proteoglycans of the extracellular environment: clues from the gene and protein side offer novel perspectives in molecular diversity and function.** FASEB J 1996, 10(5):598-614
44. Klezovitch O, Formato M, Cerchi GM, Weisgraber KH, Scanu AM – **Structural determinants in the C-terminal domain of apolipoprotein E mediate binding to the protein core of human aortic biglycan.** J Biol Chem 2000, 275(25):18913-18918
45. Iozzo RV - **Basement membrane proteoglycans: from cellar to ceiling.** Nature 2005, 6:646-656
46. Murdoch AD, Dodge GR, Cohen I, Tuan RA, Iozzo RV – **Primary structure of the human heparan sulfate proteoglycan from basement membrane (HSPG2/perlecan). A chimeric molecule with multiple domains homologous to the low density lipoprotein receptor, laminin, neural cell adhesion molecules and epidermal growth factor.** J Biol Chem 1992, 267:8544-8557



47. Cherchi GM, Coinu R, Demuro P, Sanna G, Tidore M, Tira ME, De Luca G – **Structural and functional modifications of human aorta proteoglycans in atherosclerosis.** *Matrix* 1990, 255:27-39
48. Shekhonin BV, Domogatsky SP, Muzykantov VR, Idelson GL, Rukosuev VS – **Distribution of type I, III, IV and V collagen in normal and atherosclerotic human arterial wall: immunomorphological characteristics.** *Coll Relat Res* 1985, 5(4):355-68
49. Rauterberg J, Jaeger E, Althaus M – **Collagens in atherosclerotic vessel wall lesions.** *Curr Top Pathol* 1993, 87:163-92
50. Clark JM, Glagov S – **Transmural organization of the arterial media: the lamellar unit revisited.** *Atherosclerosis* 1985, 5(1):19-34
51. Walker-Caprioglio HM, Trotter JA, Little SA, McGuffee LJ - **Organization of cells and extracellular matrix in mesenteric arteries of spontaneously hypertensive rats.** *Cell Tissue Res* 1992, 269(1):141-149
52. Farquhar MG - **The glomerular basement membrane. A selective macromolecular filter.** *Cell Biology of Extracellular Matrix*, 1991 365-418
53. Katsuda S, Okada Y, Minamoto T, Oda Y, Matsui Y, Nakanishi - **Collagens in human atherosclerosis. Immunohistochemical analysis using collagen type-specific antibodies.** *Arterioscler Thromb* 1992, 12(4):494-502
54. Bidanset DJ, Guidry C, Rosenberg LC, Choi HU, Timpl R, Hook M - **Binding of the proteoglycan decorin to collagen type VI.** *J Biol Chem* 1992, 267(8):5250-5256
55. Heller-Harrison Ra, Carter WG - **Pepsin-generated type VI collagen is a degradation product of GP140.** *J Biol Chem* 1984, 259(11):6858-6864
56. Balboni CG et Al - **Anatomia umana.** Edi-Ermes Milano, 1993
57. Schoen FJ - **Future directions in tissue heart valves: impact of recent insights from biology and pathology.** *J Heart Valve Dis* 1999, 8:350–358
58. Deck JD, Thubrikar MJ, Scheneider PJ, Nolan SP - **Structure, stress and tissue repair in aortic valve leaflets.** *Cardiovasc Res* 1988, 22:7-16
59. Torii S, Banshey RI and Nakao K - **Acid Mucopolysaccharide composition of human heart valve.** *Biochim Biophys Acta* 1965, 101:285-291
60. Sell S and Scully RE - **Aging changes in the aortic and mitral valves: histologic and histochemical studies with observations on calcific aortic stenosis and calcification of the mitral annulus.** *Am J Pathol* 1965, 46:345-365
61. Meyer K, Davidson E, Linker A and Hoffman P - **The acid mucopolysaccharides of connective tissue.** *Biochim Biophys Acta* 1956, 21:506-518
62. Moretti A and Whitehouse MW – **Changes in the mucopolysaccharide composition of bovine heart valves with age.** *Biochem J* 1963, 87(2):396-402

63. Hostrup SP, Sodian R, Daebritz S, Wang J, Bacha EA, Martin DP, Moran A, Guleserian KJ, Sperling JS, Kaushal S, Vacanti JP, Schoen FJ, Mayer JE – **Functional living trileaflet heart valves grown in vitro**. *Circulation* 2000, 102 [suppl III]:44-49
64. Schoen FJ, Levy RJ – **Tissue heart valves: current challenges and future research perspectives**. *J. Biomed Mater Res*, 1999; 47:439-465
65. Harken DF, Taylor WJ, Lefemine AA, Lunzer S, Low HB, Cohen ML, Jacobey JA – **Aortic valve replacement with a caged ball valve**. *Am J Cardiol* 1962, 9:292-299
66. Vyavahare NR, Ogle M, Schoen FJ, Zand R, Gloeckner DC, Sacks M, Levy R- **Mechanisms of bioprosthetic heart valve failure: Fatigue causes collagen denaturation and glycosaminoglycan loss**. *J Biomed Mater Res* 1999, 46:44-50
67. Lovekamp JJ, Simionescu DT, Mercuri JJ, Zubiateg B, Sacksb MS, Vyavahare NR - **Stability and function of glycosaminoglycans in porcine bioprosthetic heart valves**. *Biomaterials* 2006, 27:1507–1518
68. Schoen FJ, Levy RJ, Piehler HR – **Pathological considerations in replacement cardiac valves**. *Cardiovasc Pathol* 1992, 1:29-52
69. Edmunds LH, Clark RE, Cohn LH, Grunkemeier GL, Miller DC, Weisel RD – **Guidelines for reporting morbidity and mortality after cardiac valvular operation**. *Ann Thorac Surg* 1996, 62:932-935
70. Cannegieter SC, Rosendaal FR, Briet E – **Thromboembolic and bleeding complications in patients with mechanical heart valve prostheses**. *Circulation* 1994, 89:635-641
71. Simionescu DT, Lovekamp JJ, Vyavahare NR- **Glycosaminoglycan-degrading enzymes in porcine aortic heart valves: implication for bioprosthetic heart valve degeneration**. *The Journal of Heart Valve Disease* 2003, 12:217-225
72. Simionescu DT, Lovekamp JJ, Vyavahare NR – **Degeneration of bioprosthetic heart valve cusp and wall tissue is initiated during tissue preparation: an ultrastructural study**. *The Journal of Heart Valve Disease* 2003, 12:226-234
73. Grande-Allen KJ, Mako WJ, Calabro A, Shi Y, Ratliff NB, Vesely I – **Loss of chondroitin 6-sulfate and hyaluronan from failed porcine bioprosthetic valve**. *J Biomed Mater Res* 2003, 65A:251–259
74. Shon YH and Wolfenbarger LJ - **Proteoglycan content in fresh and cryopreserved porcine aortic tissue**. *Cryobiology* 1994, 31(2):121-132
75. Grande-Allen KJ, Osman N, Ballinger ML, Dadlani H, Marasco S, Little PJ – **Glycosaminoglycan synthesis and structure as targets for the prevention of calcific aortic valve disease**. *Cardiovascular Research* 2007, 76(1):19-28



76. Tominaga T, Kitagawa T, Masuda Y, Hori T, Kano M, Yasuta M, Katoh I – **Viability of cryopreserved semilunar valves: an evaluation of cytosolic and mitochondrial activities.** *Ann Thorac Surg* 2000, 70:792-795
77. Jen-Her L, Yen C, Wen-Hu H, Betau H, Chuh-Khium C, Chi-Chin W, Ping-Zen Y, Hsung-Hsing W - **Metabolic detriment in donor heart valves induced by ischemia and cryopreservation.** *Ann Thorac Surg* 1998, 65:24-27
78. Villalba R, Peña J, Luque E, Gómez Villagrán JL - **Characterization of ultrastructural damage of valves cryopreserved under standard conditions.** *Cryobiology* 2001, 43:81–84
79. Valente M, Faggian G, Billingham ME, Talenti E, Calabrese F, Casula R, Shumway NE, Thiene G - **The aortic valve after heart transplantation.** *Ann Thorac Surg* 1995, 60:s135-140
80. Koolbergen DR, Hazekamp MG, De Heer E, Bruggemans EF, Huysmans HA, Dion RA, Bruijn JA - **The pathology of fresh and cryopreserved homograft heart valves: an analysis of forty explanted homograft valves.** *J. Thorac Cardiovasc Surg* 2002, 124: 689-697
81. Kirklin JK, Smith D, Novick W, Naftel DC, Kirklin JW, Pacifico AD, Nanda NC, Gelmcke FR, Bourge RC - **Long-term function of cryopreserved aortic homografts.** *J Thorac Cardiovasc Surg* 1993, 106:154-165
82. Legare FJ, Lee TDG, Ross DB - **Cryopreservation of rat aortic valves results in increased structural failure.** *Circulation* 2000, 102(III):75-78
83. Dainese L, Polvani GL, Formato M, Guarino A, Biglioli P - **Cryopreservation of porcine aortic valve on open status increased matrix glycosaminoglycan structural maintenance.** *Advances in Tissue Banking* 2003, 7:485-499
84. Dainese L, Barili F, Topkara VK, Cheema FH, Formato M, Aljaber E, Fusari M, Micheli B, Guarino A, Biglioli P, Polvani G - **Effect of cryopreservation techniques on aortic valve glycosaminoglycans.** *Artificial Organs* 2006, 30(4):259–264
85. Mitchell RN, Jonas RA, Schoen FJ - **Structure-function correlations in cryopreserved allograft cardiac valves.** *Ann Thorac Surg* 1995, 60:S108-113
86. Sodian R, Hoerstrup SP, Sperling JS, Daebritz S, Martin DP, Moran AM, Kim BS, Schoen FJ, Vacanti JP, and Mayer Jr JE - **Early in vivo experience with Tissue-Engineered trileaflet heart valves.** *Circulation* 2000, 102[Suppl. III]:22-29
87. Shinoka T - **Tissue Engineered heart valves: autologous cell seeding on biodegradable polymer scaffold.** *Artificial Organs* 2002, 26[5]:402-406
88. Neuenchwander S, Hoerstrup SP - **Heart valve tissue engineering.** *Transplant Immunology* 2004, 12(3-4):359-65

89. Schmidt D, Hoerstrup SP - **Tissue engineered heart valves based on human cells.** Swiss Med WKLY 2005, 135:618–623
90. Hoerstrup SP, Kadner A, Melnitchouk S, Trojan A, Eid K, Tracy J, Sodian R, Visjager JF, Kolb SA, Grunenfelder J, Zund G, Turina MI - **Tissue engineering of functional trileaflet heart valves from human marrow stromal cells.** Circulation 2002, 106[Suppl. I]:143-150
91. Lamari FN, Militopoulou M, Mitropoulou TN, Hjerpe A, Karamanos NK - **Analysis of glycosaminoglycan-derived disaccharides in biologic samples by capillary electrophoresis and protocol for sequencing glycosaminoglycans.** Biomed Chromatogr 2002, 16(2):95-102
92. Oonuki Y, Yoshida Y, Uchiyama Y, Asari A - **Application of fluorophore-assisted carbohydrate electrophoresis to analysis of disaccharides and oligosaccharides derived from glycosaminoglycans.** Analytical Biochemistry 2005, 343:212–222
93. Lamari F, Theocharis A, Hjerpe A, Karamanos NK - **Ultrasensitive capillary electrophoresis of sulfated disaccharides in chondroitin /dermatan sulfates by laser-induced fluorescence after derivatization with 2-aminoacridone.** Journal of Chromatography B 1999, 730:129–133
94. Upreti VV, Khurana M, Cox DS, Eddington ND - **Determination of endogenous glycosaminoglycans derived disaccharides in human plasma by HPLC: validation and application in a clinical study.** J Chromatogr B 2006, 831(1-2):156-62
95. Spina M, Ortolani F, Elmesslemani A, Gandaglia A, Bujan J, Garcia-Honduvilla N, Vesely I, Gerosa G, Casarotto D, Petrelli L, Marchini M - **Isolation of intact aortic valve scaffolds for heart valve bioprostheses: extracellular matrix structure, prevention from calcification and cell repopulation features.** J Biomed Mater Res A 2003, 67[4]:1338-1350
96. Bertipaglia B, Ortolani F, Petrelli L, Gerosa G, Spina M, Pauletto P, Casarotto D, Marchini M, Sartore S - **Cell characterization of porcine aortic valve and decellularized leaflets repopulated with aortic valve interstitial cells: the VESALIO project (Vitalitate Exornatum Succedaneum Aorticum Labore Ingenioso Obtenibitur).** Ann Thorac Surg 2003, 75[4]:1274-1282
97. Bitter T, Muir HM - **A modified uronic acid carbazole reaction.** Anal Biochem 1962, 4:330-334
98. Cappelletti R, Del Rosso M, Chiarugi VP - **A new electrophoretic method for the complete separation of all known animal glycosaminoglycans in a monodimensional run.** Anal Biochem 1979, 99:311-315
99. Cherchi GM, Formato M, Demuro P, Masserini M, Varani I, DeLuca G - **Modifications of low density lipoprotein induced by the interaction with human plasma glycosaminoglycan-protein complexes.** Biochim Biophys Acta 1994, 1212:345–352

100. Theocharis AD, Theocharis DA, De Luca G, Hjerpe A, Karamanos NK - **Compositional and structural alterations of chondroitin and dermatan sulfates during the progression of atherosclerosis and aneurysmal dilatation of the human abdominal aorta.** *Biochimie* 2002, 84(7):667-674
101. Grande-Allen KJ, Calabro A, Gupta V, Wight TN, Hascall VC, Vesely I - **Glycosaminoglycans and proteoglycans in normal mitral valve leaflets and chordae: association with regions of tensile and compressive loading.** *Glycobiology* 2004, 14(7):621-633
102. Calabro A, Benavides M, Tammi M, Hascall VC, Midura RJ - **Microanalysis of enzyme digests of hyaluronan and chondroitin/dermatan sulfate by fluorophore-assisted carbohydrate electrophoresis (FACE).** *Glycobiology* 2000, 10(3):273-81
103. Zinellu A, Pisanu S, Zinellu E, Lepedda AJ, Cherchi GM, Sotgia S, Carru C, Deiana L, Formato M - **A novel LIF-CE method for the separation of hyaluronan- and chondroitin sulfate-derived disaccharides: Application to structural and quantitative analyses of human plasma low- and high-charged chondroitin sulfate isomers.** *Electrophoresis* 2007, 28:2439–2447
104. Karousou EG, Militopoulou M, Porta G, De Luca G, Hascall VC, Passi A - **Polyacrylamide gel electrophoresis of fluorophore-labeled hyaluronan and chondroitin sulfate disaccharides: application to the analysis in cells and tissues.** *Electrophoresis* 2004, 25(17):2919-2925
105. Vesely I - **Heart valve tissue engineering.** *Circ Res* 2005, 97:743–755
106. Liao J, Joyce EM, Sacks MS - **Effects of decellularization on the mechanical and structural properties of the porcine aortic valve leaflet.** *Biomaterials* 2008, 29:1065–1074
107. Gupta V, Werdenberg JA, Lawrence BD, Mendez JS, Stephens EH, Grande-Allen KJ - **Reversible secretion of glycosaminoglycans and proteoglycans by cyclically stretched valvular cells in 3D culture.** *Annals of Biomedical Engineering* 2008, 36(7):1092–1103
108. Shah SR, Vyavahare NR - **The effect of glycosaminoglycan stabilization on tissue buckling in bioprosthetic heart valves.** *Biomaterials* 2008, 29:1645-1653
109. Stephens EH, Chu CK, Grande-Allen KJ - **Valve proteoglycan content and glycosaminoglycan fine structure are unique to microstructure, mechanical load and age: relevance to an age-specific tissue-engineered heart valve.** *Acta Biomaterialia* 2008, 4(5):1148-1160
110. Seebacher G, Grasl C, Stoiber M, Rieder E, Kasimir MT, Dunkler D, Simon P, Weigel G, Schima H - **Biomechanical properties of decellularized porcine pulmonary valve conduits.** *Artificial Organs* 2007, 32(1):28–35

111. Viola M, Karousou EG, Vigetti D, Genasetti A, Pallotti F, Guidetti GF, Tira E, De Luca G, Passi A - **Decorin from different bovine tissues: study of glycosaminoglycan chain by PAGEFS**. *Journal of Pharmaceutical and Biomedical Analysis* 2006, 41:36–42
112. Karousou EG, Porta G, De Luca G, Passi A - **Analysis of fluorophore-labelled hyaluronan and chondroitin sulfate disaccharides in biological samples**. *Journal of Pharmaceutical and Biomedical Analysis* 2004, 34:791–795